

Ultrastructure, Histochemistry, and Mineralization Patterns in the Ecdysial Suture of the Blue Crab, *Callinectes sapidus*

Carolina Priester, Richard M. Dillaman,* and D. Mark Gay

Department of Biological Sciences, University of North Carolina at Wilmington, Wilmington, NC 28403-5915, USA

Abstract: The ecdysial suture is the region of the arthropod exoskeleton that splits to allow the animal to emerge during ecdysis. We examined the morphology and composition of the intermolt and premolt suture of the blue crab using light microscopy and scanning electron microscopy. The suture could not be identified by routine histological techniques; however 3 of 22 fluorescein isothiocyanate-labeled lectins tested (*Lens culinaris* agglutinin, *Vicia faba* agglutinin, and *Pisum sativum* agglutinin) differentiated the suture, binding more intensely to the suture exocuticle and less intensely to the suture endocuticle. Back-scattered electron (BSE) and secondary electron observations of fracture surfaces of intermolt cuticle showed less mineralized regions in the wedge-shaped suture as did BSE analysis of premolt and intermolt resin-embedded cuticle. The prism regions of the suture exocuticle were not calcified. X-ray microanalysis of both the endocuticle and exocuticle demonstrated that the suture was less calcified than the surrounding cuticle with significantly lower magnesium and phosphorus concentrations, potentially making its mineral more soluble. The presence or absence of a glycoprotein in the organic matrix, the extent and composition of the mineral deposited, and the thickness of the cuticle all likely contribute to the suture being removed by molting fluid, thereby ensuring successful ecdysis.

Key words: crustacean, ecdysis, lectin, molt, calcification, biomineralization, amorphous calcium carbonate

INTRODUCTION

The cuticle of the blue crab is divided into four layers. Epicuticle, the outermost layer, represents about 2% of the total cuticle thickness (Hegdahl et al., 1977b). Below the epicuticle are the exocuticle, the endocuticle, and the membranous layer, respectively (Travis & Friberg, 1963; Green & Neff, 1972; Roer & Dillaman, 1993). The exocuticle is approximately 24% of the total cuticle thickness and is calcified (Hegdahl et al., 1977a, 1977b). It has a tanned, chitin-protein matrix arranged in lamellae (Green & Neff, 1972). Both epi- and exocuticle are deposited during premolt and are calcified postecdysis (Hegdahl et al., 1977a, 1977b). Endocuticle, which constitutes approximately 74% of total cuticle thickness, is not tanned and has a chitin-protein matrix also arranged in lamellae (Dennell, 1947; Travis, 1955a; Hegdahl et al., 1977c; Giraud-Guille, 1984b). This layer is calcified as it is being deposited and becomes as heavily calcified as the epicuticle and exocuticle (Green & Neff, 1972; Hegdahl et al., 1977a, 1977c). The mineral in these three layers is calcium carbonate (CaCO₃) in the form

of calcite (Travis, 1963; Simkiss, 1975). The membranous layer is the innermost layer, and it also has a chitin-protein matrix. However, it is neither calcified nor tanned (Green & Neff, 1972). The cuticular layers contain chitin and protein and have been demonstrated by Marlowe et al. (1994) to also contain additional glycoproteins and carbohydrate residues.

Underneath the four layers of cuticle is the hypodermis (epithelial tissue) (Travis, 1955a, 1955b; Travis, 1957; Travis, 1965; Roer & Dillaman, 1984) that is responsible for secreting the new cuticle as well as the molting fluid (Travis, 1955a, 1955b, 1957, 1965; Neville, 1975; Skinner, 1985; O'Brien & Skinner, 1987, 1988; Spindler-Barth et al., 1990). As the cuticle is deposited, the hypodermis leaves behind in the cuticle numerous small, branching cytoplasmic extensions, called pore canals (Green & Neff, 1972; Hegdahl et al., 1977a, 1977c; Compère & Goffinet, 1987a, 1987b). Supposed imprints of the margins of the hypodermal cells, interprismatic septa (IPS), are also found in the exocuticle and are thought to be the initial sites of calcification (Travis, 1957, 1963, 1965; Hegdahl et al., 1977a; Giraud-Guille, 1984a; Hequembourg, 2002).

To grow, crustaceans replace their exoskeleton in a series of events called the molt cycle. The molt cycle has been divided into five stages (A–E) by Drach (1939), with

stages based on cuticle hardness or softness in certain anatomical regions (Drach, 1939; Travis, 1955a; Stevenson, 1968). The physiological, biochemical, and histological changes during those stages have been extensively examined (Travis, 1955a, 1955b, 1957; Johnson, 1980; Roer & Dillaman, 1984; Mangum et al., 1985; Spindler-Barth et al., 1990; Shafer et al., 1995). Also examined has been the pattern of calcification in the new cuticle (Skinner, 1962; Travis, 1963, 1965; Travis & Friberg, 1963; Giraud-Guille, 1984a; Hequem-bourg, 2002; Dillaman et al., 2005).

The intermolt or C_4 stage, in which crustaceans spend most of their time, is characterized by the cuticle being completely deposited and fully mineralized (Green & Neff, 1972; Mangum, 1985). Following intermolt is stage D_0 , which is activated by crustecdysone, a molting hormone (Freeman, 1980). During D_0 the hypodermis separates from the cuticle (apolysis). Separation is caused by secretion from the hypodermis into the ecdysial space of a molting fluid containing digestive, chitinolytic enzymes including chitinase, chitobiase, and *N*-acetyl- β -*D*-glucosaminidase (Green & Neff, 1972; Neville, 1975; O'Brien & Skinner, 1987, 1988; Spindler & Buchholz, 1988; Buchholz, 1989; Spindler & Funke, 1989; Spindler-Barth et al., 1990; Compère et al., 1998; Roer et al., 2001). These enzymes promote the partial dissolution of the innermost, noncalcified membranous layer of the old cuticle (Skinner, 1962, 1985) and subsequently the partial degradation of the calcified layers (Compère et al., 1998). Molting crabs partially resorb the products of the digestion of their old exoskeleton (Spindler & Buchholz, 1988; Compère et al., 1998) and underneath it deposit a new larger, flexible exoskeleton.

From stage D_1 through D_3 , while the new cuticle is being formed, the old cuticle is continuing to be digested (Passano, 1960; Green & Neff, 1972; Stevenson, 1972). By the end of stage D_3 skeletal resorption is at its maximum (Passano, 1960), and the cuticle begins to split at predictable and externally visible sites, the sutures (Green & Neff, 1972). Just prior to ecdysis, at stage D_4 (Green & Neff, 1972), the cuticle suture opens in response to expansion of the underlying new cuticle (Passano, 1960; Mangum et al., 1985). The suture has been referred to as ecdysial lines or clefts, or lines of weakness or dehiscence, and its degree of weakness aids in premolt stage classification (Passano, 1960; Green & Neff, 1972; Mangum, 1985; Compère et al., 1998). The dorsal carapace remains attached at the anterior margin, therefore acting as a hinge. As the posterior and lateral margin open, the crab backs out of its old dorsal carapace and attached structures. At ecdysis (stage E) the crab emerges from the old exoskeleton and rapidly takes up additional water in order to fully expand its carapace (Passano, 1960; Green & Neff, 1972; Mangum et al., 1985). Immediately after ecdysis the crab's exoskeleton is uncalcified so it relies on a hydrostatic skeleton for support and movement (Taylor & Kier, 2003).

Whereas the role of the suture in crustaceans has been described previously, its ultrastructure and mechanism for

splitting have not been investigated in depth. The only reports of suture ultrastructure and composition are for insects (Chapman, 1982; Kathirithamby et al., 1990; Hadley, 1994). However, because the cuticle of crustaceans is composed of the same number of layers as the cuticle of insects (Neville, 1975; Hadley, 1994), comparisons between insects and crustaceans can be useful. In the small number of insects where it has been examined, the cuticle at the suture has been shown to be different from the adjacent cuticle. For example, Chapman (1982) demonstrated that in larval hemimetabolous insects the exocuticle is absent at the suture line; only endocuticle and epicuticle are present. Supposedly endocuticle is preferentially digested by molting fluid and a line of weakness is formed. However, Kathirithamby et al. (1990) report that in the puparium cap of *Elenchus tenuicornis* (Insecta: Strepsiptera) all the layers, including exocuticle, are present at the suture. In this case the exocuticle is untanned, thereby rendering it different from the adjacent exocuticle and more easily digested by molting fluid. This would leave the carapace attached only at the epicuticle, thereby forming a line of weakness (Kathirithamby et al., 1990).

Crustacean cuticle differs from insect cuticle in several aspects. For example, crustaceans mineralize many portions of their cuticle (Drach, 1939; Passano, 1960; Green & Neff, 1972; Giraud-Guille, 1984a; Roer & Dillaman, 1984; Hequem-bourg, 2002) whereas insect cuticle is generally not calcified. One exception to this is the fly larva *Exeretonevra angustifrons*, whose cuticle has been found to contain amorphous calcium phosphate (Rasch et al., 2003). However, like the ultrastructure of the suture line in crustaceans, the calcium content of the suture has never been measured. Neither have the magnesium and phosphorus levels been measured. Those values may be important because both can affect the solubility of the mineral when they are substituted in the CaCO_3 lattice (Simkiss, 1994; Raz et al., 2000). A difference in ultrastructure, calcium content, or mineral solubility between the suture line and the adjacent cuticle might explain why this region is preferentially digested by the molting fluid, a solution released into the space between the old and new cuticle and containing, but not limited to, chitinases and chitobiases (Compère et al., 1998; Roer et al., 2001). Conversely, it could simply indicate that this region is mechanically weaker, thus splitting when internal pressure increases due to water uptake by the underlying tissue prior to ecdysis.

The objective of this investigation is to describe the functional morphology and mineral distribution of the suture line in the blue crab, *Callinectes sapidus*, using scanning electron microscopy and light microscope histochemistry. Four hypotheses were tested concerning the structure, composition, mineral content, and dimensions of the suture. The first hypothesis was that the ventral suture line morphology does not vary from that of the cuticle surrounding it. The second hypothesis was that the organic matrix of the suture line of crustaceans has the same morphology and

composition as the adjacent cuticle. The third hypothesis was that the mineral content and composition of the suture does not vary from that of the surrounding cuticle. The fourth and final hypothesis was that the suture dimensions do not vary across regions, these regions being the anterior, middle, and posterior portions of the carapace.

MATERIALS AND METHODS

Animals and Experimental Design

Immature female blue crabs, 5–11.8 cm in carapace width, were obtained from Endurance Sea Food, Kill Devil Hills, NC, or Scott Rader, Wilmington, NC. Crabs were collected at intermolt, stage C₄, and premolt, stages D₀ through D₄ (Drach, 1939). From each individual several adjacent pieces were cut from the ventral side of the carapace that included the ecdysial suture and approximately 5 mm of adjacent cuticle on each side of the suture.

Light Microscopy

Cuticle samples were collected and fixed in Bouin's fixative (Presnell & Schreiberman, 1997) or in alcoholic formalin (9:1) (Marlowe et al., 1994). Pieces were fixed for 5 days, with a change of the fixatives after the first 24 h. Pieces fixed in alcoholic formalin were decalcified in 10% EDTA in 0.1 M Tris buffer, pH 7.6, for 2 weeks or until they were flexible. Samples were then rinsed in 0.1 M Tris buffer, pH 7.6, dehydrated through an ascending series of ethanol, cleared in toluene, and embedded in paraffin. Sections 8 μm thick were attached to slides with Mayer's egg white albumin (Presnell & Schreiberman, 1997), except for sections to be stained with acridine orange and lectins. Lectin and acridine orange staining followed the techniques described by Marlowe et al. (1994) and Marlowe and Dillaman (1995), respectively.

Tissues were stained with periodic acid—Schiff (PAS) stain, hematoxylin and eosin (H&E), 0.1% toluidine blue in 0.2 M sodium borate buffer, pH 9.2 (Presnell & Schreiberman, 1997), paraldehyde fuchsin (PAF) (Gomori, 1950; Thompson, 1966), or fluorescein isothiocyanate (FITC) labeled lectins. Tissues fixed in alcoholic formalin were also stained with acridine orange (Marlowe & Dillaman, 1995). Preliminary studies were performed using a battery of 21 fluorescent-labeled lectins previously used by Marlowe et al. (1994). When two of these lectins, *Lens culinaris* agglutinin (LCA) and *Pisum sativum* agglutinin (PSA) (Vector Laboratories, Inc., Burlingame, CA), showed differential binding between the suture line cuticle and the adjacent cuticle, another lectin with similar binding affinity was chosen and used. This third lectin was *Vicia faba* agglutinin (VFA) (EY Laboratories, Inc., San Mateo, CA). All three have been reported to bind to fucosylated α -N-acetylglucosamine with mannose dendrimers (Debray et al., 1981; Young et al., 1996). Lectins were used in a concentration of 30 $\mu\text{g}/\text{ml}$ in

crab physiological saline solution (Roer, 1980). Five hundred microliters of the diluted lectin were used to stain each slide. Samples stained with acridine orange or FITC-labeled lectins were observed with an Olympus BH-2 epifluorescence microscope with blue excitation achieved by using a DM500 dichroic mirror with an IF490 excitation filter and a 515-nm barrier filter. Images were collected with a Spot RT digital color camera (Diagnostic Instruments, Inc., Sterling Heights, MI).

Scanning Electron Microscopy

Cuticle containing the suture line was obtained by cutting along side the suture line with a Dremel cutting tool (Dremel, Robert Bosch Tool Corp., Mount Prospect, IL). Approximately 5 mm were left on each side of the suture line to prevent destruction of the region of interest and to allow surrounding cuticle for comparison to the cuticle of the suture line. From one side of each crab the piece was allowed to air dry. From the other side of each crab the piece was freeze-dried. The freeze-dried pieces were fractured into smaller pieces. Air-dried samples were mounted on aluminum stubs with colloidal graphite, coated with 6 nm of platinum–palladium (80:20) in a Cressington 208 HR Sputter Coater (Cressington Scientific, Inc., Cranberry Twp., PA). Some pieces were mounted for cross-sectional view, others for internal or external view of the suture. Samples were observed with the secondary electron (SE) and back-scattered electron (BSE) modes of the Philips XL30 S FEG scanning electron microscope (SEM) as well as nondispersive X-ray microanalysis (Phoenix, EDAX Inc., Mahwah, NJ). Sample surfaces were normal to the BSE detector. The X-ray mode allowed both mapping and quantification of specific elements in the samples.

Features revealing cuticle structure were best observed in samples fractured after freeze drying or air drying, whereas, to obtain a smooth surface for X-ray mapping, freeze-dried samples were embedded in Spurr's epoxy resin (Spurr, 1969), cut, and polished. The suture line could be seen through the translucent resin block, so nicks were made on the face of the resin on either side of the suture so that its location in the resin block could be precisely determined when the sample face was viewed in the SEM. Pieces of cuticle or cuticle in resin were attached to aluminum stubs with colloidal graphite so that a cross section of the suture with adjacent cuticle on either side was visible. Samples were coated with 6 nm of platinum–palladium (80:20) and then each sample was observed with the SEM, utilizing SE, BSE, and Phoenix EDAX nondispersive X-ray microanalysis modes at 10 kV accelerating voltage. The backscattered images were collected in the compositional mode at 10 kV with an annular solid state detector mounted under the pole piece. The elemental composition of the samples was determined using the EDAX ZAF Quantification (Standardless) X-ray microanalysis mode. Areas of interest 40 μm by 40 μm were selected and analyzed for

Figure 1. Fluorescence images of intermolt (C_4) cuticle containing the suture (arrowhead) stained with (a) acridine orange and of intermolt cuticle regions containing the suture, fixed in alcoholic formalin and stained with (b) FITC-labeled *Lens culinaris* agglutinin (LCA), (c,d) FITC-labeled *Pisum sativum* agglutinin (PSA), or (e) unstained to serve as a control. en: endocuticle; ep: epicuticle; ex: exocuticle; h: hypodermis; m: muscle; ml: membranous layer. Arrows in b and c: suture region in the endocuticle; arrowheads in b and c: suture region in the exocuticle; en: endocuticle; ex: exocuticle; arrowhead in c: prism; arrowhead in d: epicuticle.

element content at the slowest scan rate in different regions of the cuticle, including exocuticle at suture line, exocuticle at adjacent cuticle, upper (outermost) and lower (innermost) endocuticle at suture line, and endocuticle at adjacent cuticle (Fig. 4a, below). If the region of the lower endocuticle had been digested away, an area immediately above it was sampled. When the digestion reached the upper endocuticle, no measurements could be taken for the lower endocuticle, consequently reducing the sample size for this region. Weight percent and atomic percent of the elements present in the sample were recorded and ratios of elements were calculated. Because the ratios were greater than one, no transformation for the data was required.

Data were analyzed using single factor analysis of variance—Tukey multiple comparison test with unequal sample sizes (Zar, 1999), the factor being the region of the cuticle. Data were sorted and graphed in Sigma Plot 8.0 (SPSS, Inc., Plover, WI). For each sample, comprehensive elemental maps of the entire region containing both calcified cuticle and suture were obtained to investigate the spatial distribution of selected elements that were found in the square regions of the suture and adjacent cuticle that were analyzed. These elements were calcium, carbon, chloride, magnesium, sodium, oxygen, phosphorus, and sulfur. The maps were collected at 512×400 resolution, dwell time 100 ms, amplifier time $50 \mu\text{s}$, and 128 frames. Suture and adjacent cuticle thickness were measured from the micrographs of the embedded samples. Measurements of the cuticle were taken from cross sections of resin-embedded samples and were assessed using a three-way factorial analysis of variance (ANOVA) with cuticle region (suture or adjacent calcified cuticle), carapace measurement location (anterior, middle, or posterior), and stage of the molt cycle (C_4 , D_1 , or D_2) as main effects. Statistical significance of each of the main effects and interaction terms was evaluated using alpha (α) of 0.05. Significant differences in carapace thickness among measurement locations and molt stages were based on Tukey HSD post hoc comparisons (Zar, 1999).

RESULTS

Histochemistry

Staining of intermolt, C_4 , cuticle with acridine orange in a region that contained the suture and adjacent calcified cuticle (Fig. 1a) clearly differentiated the four cuticle layers,

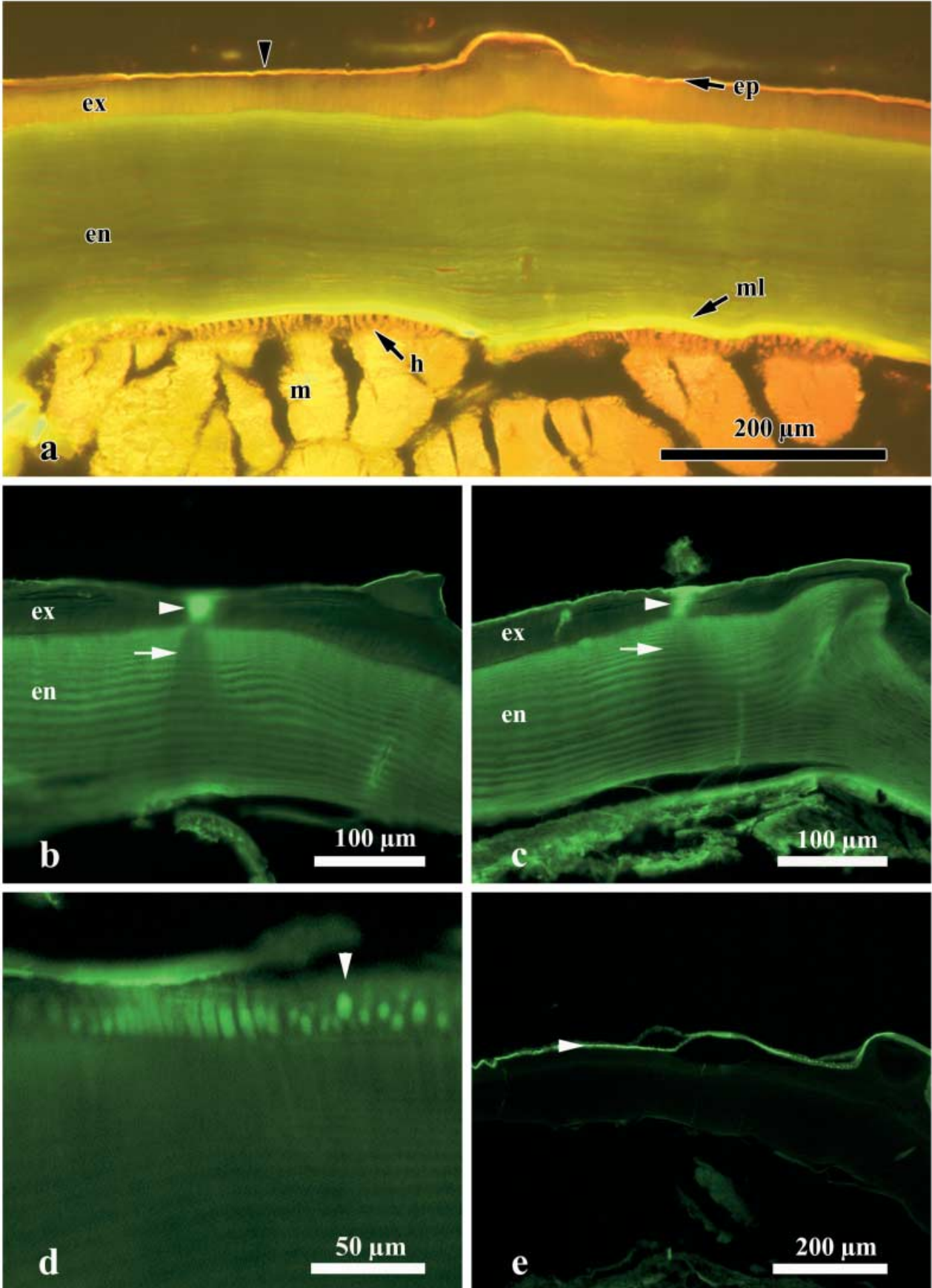
but not the suture itself. The epicuticle stained bright orange, whereas the exocuticle stained less intensely orange. The endocuticle stained green and the membranous layer stained bright chartreuse. Hypodermis and muscle could also be seen underneath the cuticle. Sections stained with H&E, PAS (with and without amylase treatment), PAF, and toluidine blue differentiated various layers of the cuticle, but did not show any differential staining of the suture as compared to the adjacent calcified cuticle. In all of the sections, the lamellae within the exocuticle and endocuticle could be easily observed and no discontinuities were apparent between the suture and the adjacent calcified cuticle. The lamellae of the suture cuticle appeared to be continuous with the lamellae of the adjacent calcified cuticle.

Lectin Affinity

Of the 22 fluorescent-labeled lectins used to stain the intermolt cuticle, only three demonstrated differential binding between the suture and the adjacent cuticle. These lectins were LCA, PSA, and VFA. All three lectins (only two shown) revealed the suture shape to be trapezoidal (Fig. 1b,c). The three lectins bound to the suture region of the exocuticle (Fig. 1b,c), staining it much more intensely than the adjacent exocuticle. The suture region of the endocuticle, however, was more lightly stained than the adjacent endocuticle, forming a trapezoid with sides at approximately a 45° angle. The distal end where it met the exocuticle was approximately $40 \mu\text{m}$ and the proximal end where it met the membranous layer was approximately $75 \mu\text{m}$. In some sections (Fig. 1d) the prisms in the adjacent exocuticle, especially at the proximal end where they met the endocuticle, also stained more intensely than other regions of the exocuticle, particularly the interprismatic septa (IPS). Sections fixed in alcoholic formalin (Fig. 1b,c,d) stained more intensely than sections fixed in aqueous Bouin's (data not shown). This influence of fixation on lectin affinity was most pronounced in sections stained with VFA, where the lectin did not bind to the cuticle fixed in aqueous Bouin's, thus making it indistinguishable from the unstained controls (Fig. 1e). In the controls, the epicuticle, including setae, demonstrated autofluorescence, whereas the remainder of the cuticle did not.

Scanning Electron Microscopy

An external (Fig. 2a,c) and internal (Fig. 2b) view of the suture, using the SE mode, showed that there is a shallow



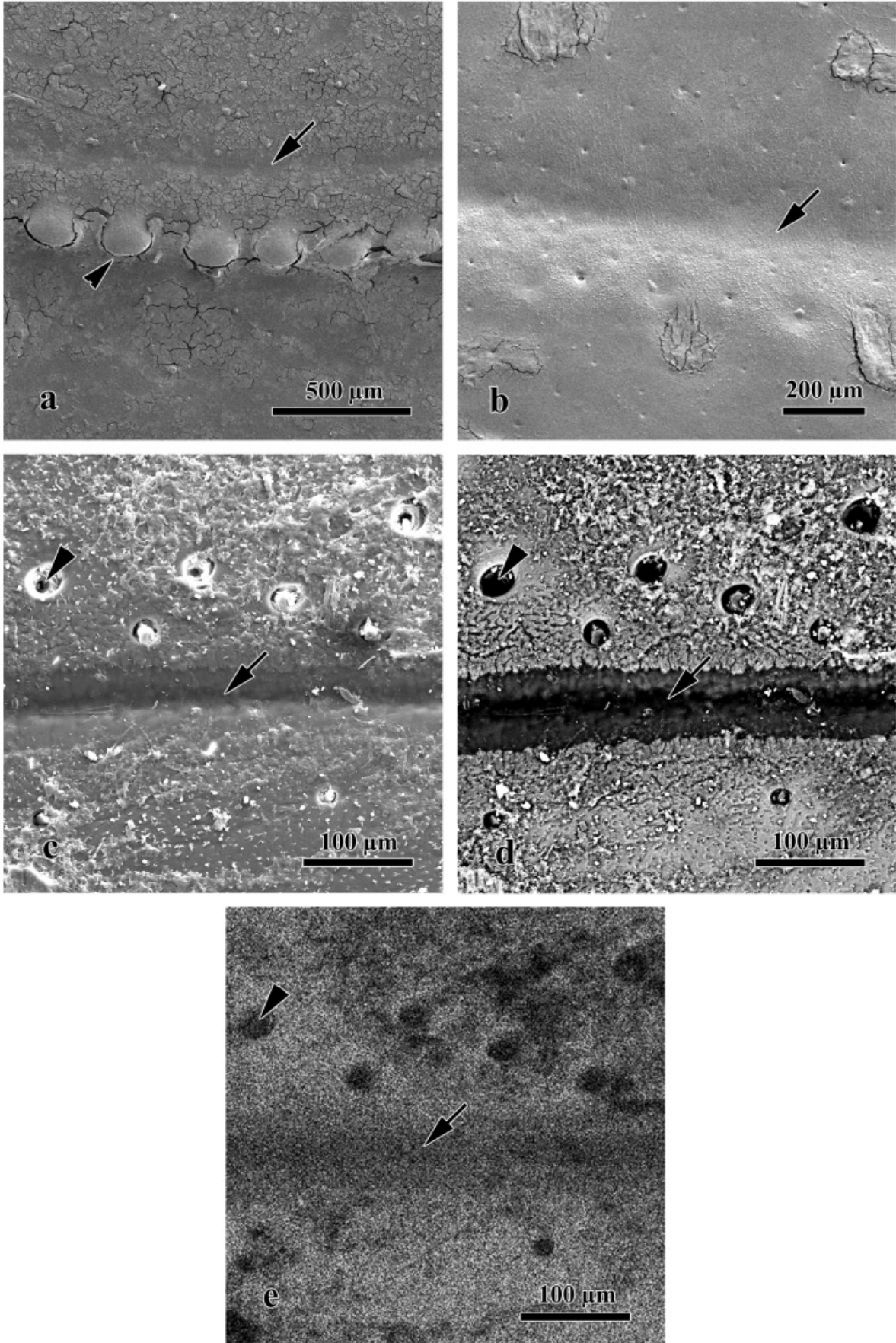


Figure 2. SEM micrographs of the suture region (arrows) of an intermolt cuticle showing external (a,c,d,e) and internal (b) surfaces. Micrographs a, b, and c are SE, d is BSE, and e is a calcium X-ray map. Micrographs a and b are from the anterior aspect of the carapace, whereas c, d, and e are from the posterior. Externally, a series of knobs forming a ridge (arrowhead in a) parallels the suture, except at the posterior aspect of the carapace (c, d, e). Canals containing receptors (arrowhead in c, d, e).

groove in the intermolt cuticle in the region of the suture, thereby making it slightly thinner than the adjacent cuticle. Externally, on the anterior ventral branchial lobe of the carapace, a series of knobs formed a ridge that often paralleled the suture (Fig. 2a). Unlike the cuticle surrounding the suture region, no setae were seen over the suture (Fig. 3a). The internal, or proximal, surface of the cuticle (Fig. 2b) had a smooth texture, possibly due to organic matter dried on the surface. The suture was only a shallow depression, just barely below the surface of the adjacent calcified cuticle. The external and internal aspects of the suture were observed in the cuticle of intermolt crabs and five premolt stages, and there were no obvious differences in its appearance among the different stages using the SE mode. In contrast, imaging with the BSE mode clearly indicated that the suture region was less mineralized (Fig. 2d). That is, the cuticle adjacent to the suture had a stronger backscattered electron signal and presumably a higher atomic number. Both BSE and SE images showed that the margin was slightly scalloped (Fig. 2c,d). The suture gradually decreased in brightness from the margins to the dark center (i.e., had a very weak BSE signal; Fig. 2d). In contrast, canals containing receptors that pass through the entire cuticle (Fig. 2c,d,e) had an even weaker BSE signal in their center. Calcium X-ray maps (Fig. 2e) showed lower calcium concentrations in the suture than the adjacent cuticle with the exception of the receptor canals that contained very low calcium concentrations.

Fracture surfaces of intermolt cuticle observed using the SE and BSE mode of the SEM in cross section showed that the cuticle layers of the suture are contiguous with those of the adjacent cuticle (Fig. 3a,b). The suture was visible and had no setae (Fig. 3a). Prisms and IPS (Fig. 3b,d) at the suture exocuticle and its vicinity were distinguishable, with the septa being brighter than the prisms, indicating that they were more mineralized. Observations with the BSE mode revealed that the prisms of the exocuticle in the suture were not in-filled with mineral (Fig. 3b,d). However, the prisms adjacent to the suture were progressively more in-filled with mineral from their distal to proximal margins, thereby forming a wedge of less calcified exocuticle (Fig. 3b). Still farther away from the center of the suture, the exocuticle appeared much more solid, with the prisms almost completely in-filled with mineral (Fig. 3b). However, some prisms were not completely in-filled near the interface of the exocuticle with the endocuticle. A higher magnification

of the exocuticle near the suture (Fig. 3c,d) showed unmineralized prisms surrounded by mineralized IPS. No noticeable difference in the structure or mineral content between the suture region of the endocuticle and the adjacent calcified endocuticle could be detected in these fractured samples (Fig. 3b).

Observation of the resin-embedded and polished samples with BSE mode (Figs. 4, 5) revealed that the exocuticle of the suture was less mineralized than the adjacent exocuticle. More specifically, the prisms were not in-filled with mineral in the region of the suture. Prisms farther away from the suture gradually were increasingly more in-filled with mineral, forming a visible wedge with a trapezoidal cross section (Fig. 4e). Endocuticle at the suture also appeared less mineralized than the adjacent endocuticle. It formed a wedge pattern as well, with sides at a 45° angle, narrower (approximately 40 μm) at the distal end and wider (between 100 μm and 250 μm, approximately) at the proximal end. There was a noticeable difference in the width of this trapezoid among anterior, middle, and posterior pieces of cuticle from the same crab (Fig. 4). In posterior pieces of cuticle the wedge was wider, measuring approximately 100 μm in the center of the endocuticle. In middle pieces the wedge measured approximately 50 μm and in anterior pieces the wedge was only 30–40 μm wide. In crabs from later premolt stages (Fig. 5a–f), closer to ecdysis, the suture region of the endocuticle appeared even less mineralized and more digested at the inner portions of the cuticle in the same wedge pattern. Digestion advanced further up into the cuticle of the suture as the crab approached ecdysis (Fig. 5, cf. a,c,e with b,d,f). Prior to digestion and demineralization, the suture and the adjacent cuticle's inner surface were almost on the same plane at stage C₄, with the suture just barely below the surface of the calcified adjacent cuticle (Fig. 4a,c,e). Digestion of matrix and demineralization progressed through the premolt stages with digestion removing the inner portions of the endocuticle across the entire cuticle, but preferentially at the suture. Digestion and demineralization followed the less calcified wedge-shaped region seen in BSE micrographs (Figs. 4, 5) forming a deeper groove and thus making the suture even thinner as compared to the adjacent cuticle (Fig. 6a). By stage D₃ virtually the entire endocuticle region of the suture was digested allowing the carapace to split. This digestion and demineralization pattern differed spatially, with the posterior showing more pronounced demineralization and

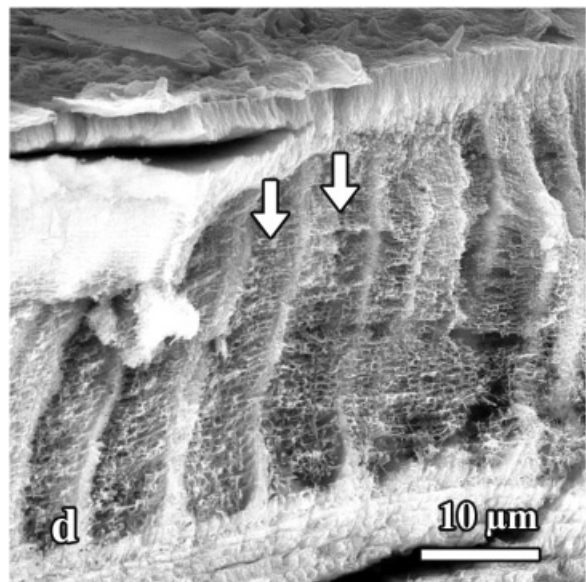
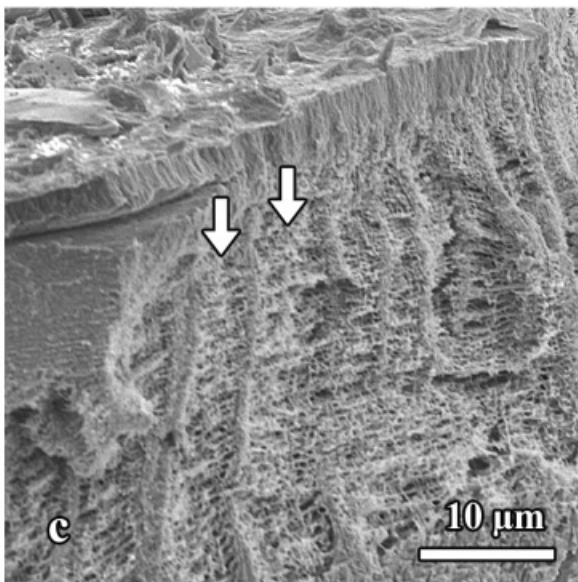
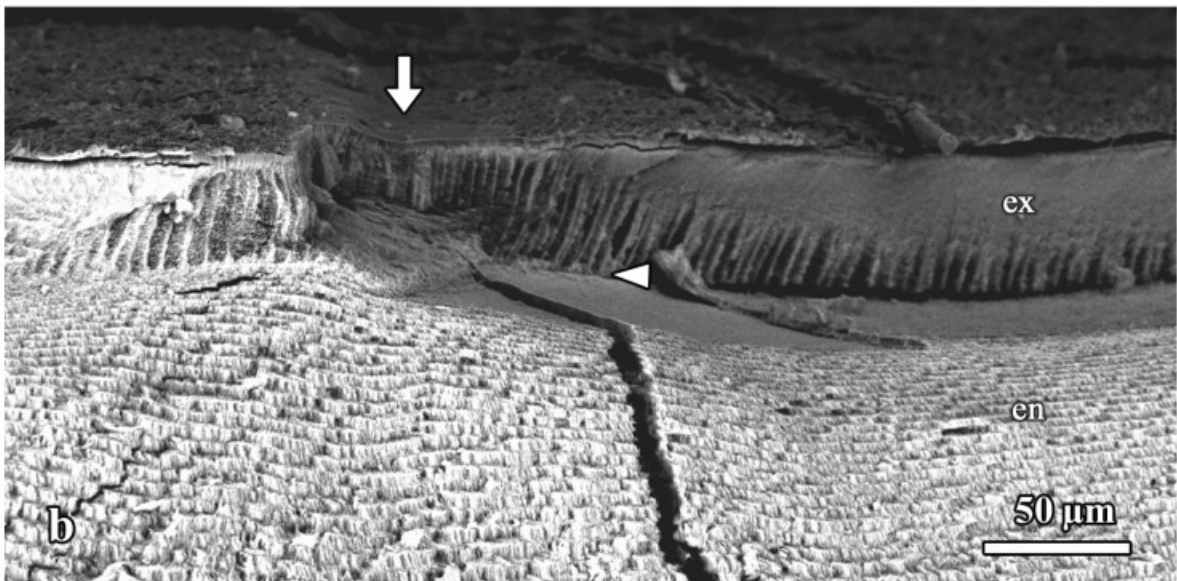
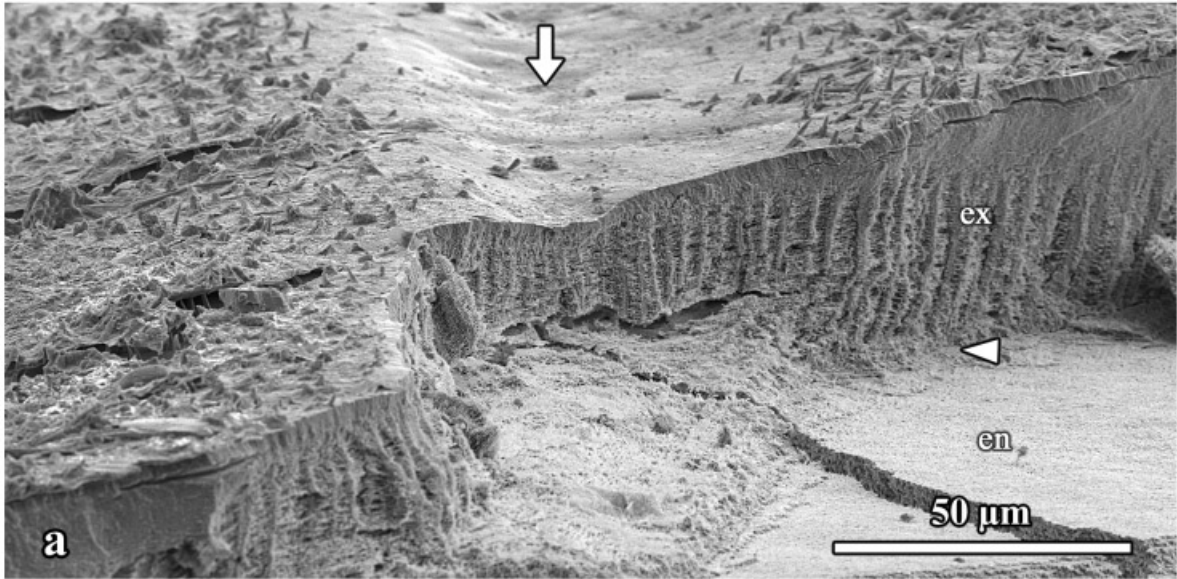


Figure 3. SEM micrographs of fractured cuticle samples from posterior sectors of the carapace of intermolt crabs. Micrographs **a** and **c** are SE, **b** and **d** are BSE. **a,b**: Exocuticle containing the entire suture (arrow). **c,d**: High magnification of the exocuticle at the suture. Arrows (**a,b**), suture; arrows (**c,d**), prisms; arrowheads (**a,b**), interface of exocuticle (ex) and endocuticle (en).

digestion than the anterior and middle sections (cf. Fig. 4e,f and Fig. 5e,f). Posterior regions also appeared to start demineralizing and being digested earlier than the other two regions sampled, so the suture cuticle was removed to a greater extent in posterior pieces. Demineralization seemed to precede digestion of the organic matrix, resulting in a layer on the inner surface of the cuticle that was detectable in BSE images (Fig. 5c,e) because it had an average atomic number closer to that of the resin than the calcified cuticle. A difference in thickness of the cuticle was also noted among anterior, middle, and posterior regions. A summary of cuticle thickness as a function of cuticle region, carapace measurement location, and stage of the molt cycle is shown in Figure 6. Mean cuticle thickness was significantly lower in the suture region compared to the adjacent calcified cuticle region ($p < 0.0001$; Fig. 6a) and cuticle thickness was greatest in the anterior sector of the carapace ($p < 0.0001$; Fig. 6b). The cuticle from stage D₂ crabs was significantly thinner ($p < 0.0001$) than cuticle from either C₄ or D₁ crabs (Fig. 6c). The interaction between cuticle region and stage of the molt cycle was also significant ($p = 0.0218$), with cuticle thickness varying among molt cycle stages in the suture region, but remaining constant across molt cycle stages in the adjacent calcified cuticle region.

X-ray Microanalysis

Elements measured in the selected sampling regions were carbon, oxygen, sodium, magnesium, phosphorus, platinum (due to coating), sulfur, chloride, palladium (due to coating), and calcium. Figure 7, b–f, shows a representative set of elemental maps for calcium, magnesium, phosphorus, oxygen, and carbon for a posterior piece of cuticle from an intermolt (C₄) crab. The same wedge pattern for the suture seen in the BSE images (Figs. 4, 5, 7a) was observed in the calcium map (Fig. 7b). A similar but much less distinct pattern was seen in the magnesium (Fig. 7c) and oxygen (Fig. 7e) maps. For the carbon map (Fig. 7f) the pattern was the same shape but reversed, with a stronger signal in the wedge-shaped suture region. For phosphorus the wedge pattern was not observed; rather, phosphorus appeared more concentrated in the exocuticle nonsuture (Fig. 7d) than in the other regions.

Quantitative analysis of the selected cuticle regions revealed that there were significant differences in the calcium concentrations of the five regions (Tables 1, 2), except between endocuticle nonsuture and exocuticle nonsuture

($p > 0.05$; Table 2), which contained the greatest concentrations of calcium. Upper endocuticle of the suture had the third greatest concentration of calcium (17.29 ± 2.89 wt%), followed by exocuticle of the suture (13.15 ± 3.61 wt%). Lower endocuticle of the suture had the lowest concentrations of calcium (10.38 ± 7.44 wt%) and the highest variance, with values ranging from 0.56 to 18.29 wt%. The region with the next highest variance was exocuticle suture (13.15 ± 3.61 wt%) with values ranging from 7.77 to 22.08 wt%.

There were also significantly different concentrations of magnesium among all the regions of the cuticle analyzed (Tables 1, 2), except between upper endocuticle suture and exocuticle suture ($p > 0.05$), which had the second lowest concentrations of magnesium (Table 1). Lower endocuticle of the suture had the lowest concentration of magnesium (0.66 ± 0.45 wt%), whereas exocuticle nonsuture had the greatest concentration of magnesium (1.75 ± 0.24 wt%), followed by the endocuticle nonsuture (1.31 ± 0.14 wt%).

Phosphorus concentrations were not significantly different among regions (Table 2), except for the exocuticle nonsuture (Tables 1, 2), which contained a significantly higher concentration of phosphorus than any other region (2.90 ± 0.50 wt%). Endocuticle nonsuture and exocuticle nonsuture oxygen concentrations were the highest (Table 1) and did not differ significantly from each other (Table 2). Lower endocuticle of the suture and exocuticle of the suture had the lowest oxygen concentrations (Table 1) and did not differ significantly from each other (Table 2) whereas upper endocuticle of the suture differed significantly from all the other regions, having an intermediate oxygen concentration (23.00 ± 2.53 wt%).

The carbon map had a pattern opposite that of calcium, with carbon concentrations being lowest in the endocuticle nonsuture and exocuticle nonsuture (Table 1), which were not significantly different from each other (Table 2). Lower endocuticle of the suture and exocuticle of the suture had the greatest amounts of carbon (Table 1) and did not differ significantly from each other (Table 2), whereas upper endocuticle of the suture differed significantly from all the other regions (Table 2), having an intermediate carbon concentration (43.62 ± 5.54 wt%).

Because Ca/Mg and Ca/P ratios have been shown to influence the solubility of calcium salts (Reddy & Nancollas, 1976; Stumm & Morgan, 1981), those ratios were examined in this study. Scatter plots of calcium concentrations versus magnesium concentrations (Fig. 8) and calcium versus phos-

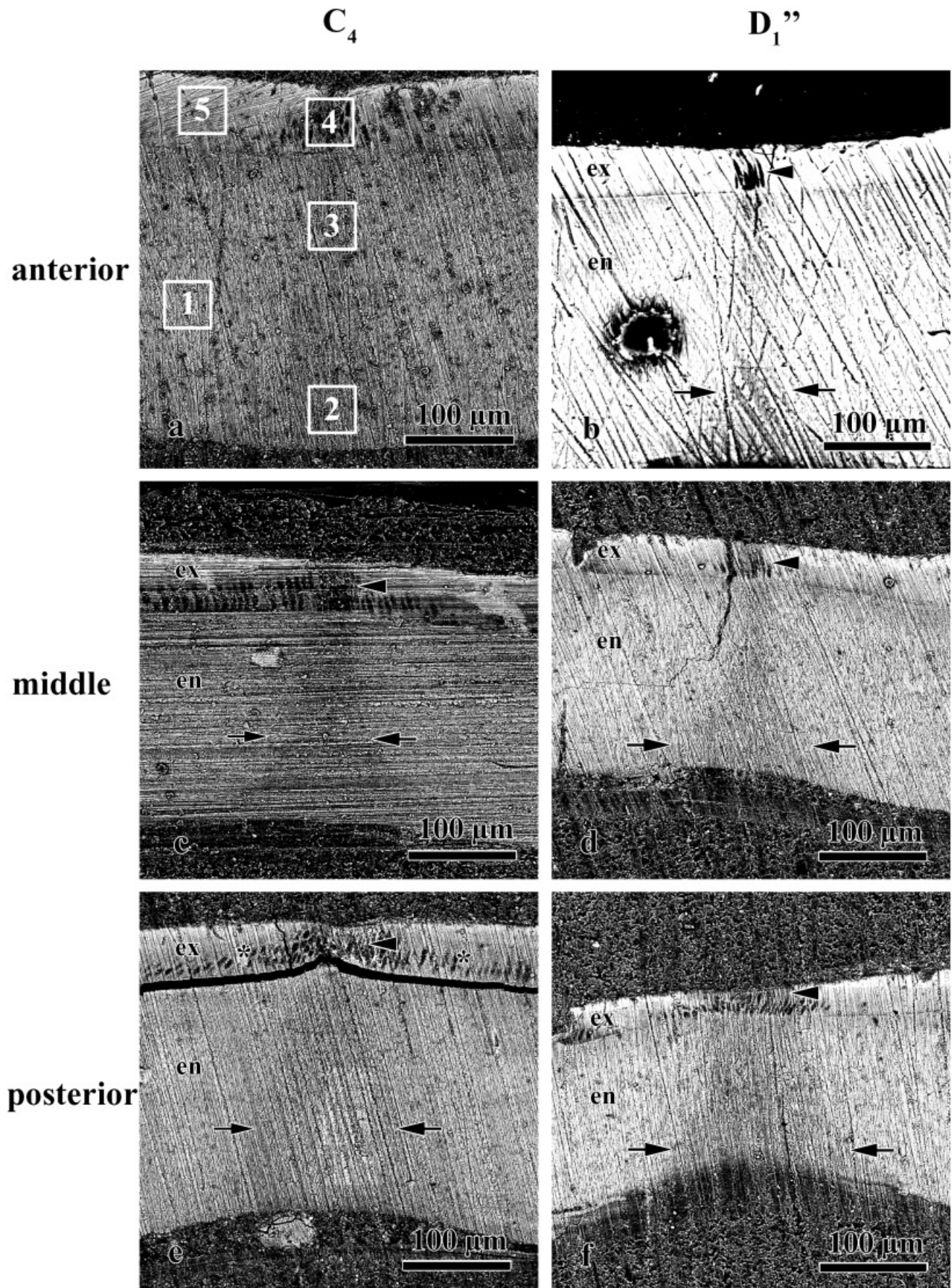


Figure 4. BSE micrographs of embedded and cut samples containing the suture of crabs in intermolt and D₁ stages. Numbered boxes in **a** exemplify the regions of the cuticle that were analyzed in each sample: 1: Endocuticle nonsuture, 2: lower endocuticle suture, 3: upper endocuticle suture, 4: exocuticle suture, and 5: exocuticle nonsuture. Arrows: suture region of the endocuticle; arrowheads: suture region of the exocuticle; *: prisms; en: endocuticle; ex: exocuticle.

phorus concentrations (Fig. 9) revealed both the relative ratios of the two elements in different regions of the cuticle and the patterns of variability within those regions. Mean ratios of calcium to magnesium and phosphorus are shown in Tables 3 and 4 as well as a summary of statistical analyses comparing values among the various regions. As seen in Figures 8 and 9, the distribution of values for each region analyzed clustered in separate groups for each region, forming distinct patterns. The calcium versus magnesium plot (Fig. 8) showed that the endocuticle nonsuture and the exocuticle nonsuture had comparable calcium concentrations but significantly different magnesium concentrations (Table 2), therefore resulting in significantly different Ca/Mg ratios (Table 3). Ratios of calcium to magnesium for the exocuticle nonsuture were the lowest and were significantly different from all other regions except the lower endocuticle suture (Table 3). The ratios of calcium to magnesium among the selected regions were highest for the endocuticle nonsuture and upper endocuticle of the suture, which were not significantly different from each other (Table 3). The upper endocuticle suture values were loosely clustered (Fig. 8), represented less calcium and magnesium than the endocuticle nonsuture, but had the same ratio of calcium to magnesium as found in the endocuticle nonsuture (Table 3). Values for the suture region of the exocuticle and lower endocuticle overlapped, except for a few values for lower endocuticle suture that had both low calcium and magnesium concentrations. Both regions had an intermediate Ca/Mg ratio and were not significantly different from one another (Table 3). There was generally a positive relationship between calcium and magnesium concentrations; as the first increased, the second one increased as well (Fig. 8). Analysis of regions containing only resin served as controls and showed a tight cluster of values close to zero for both calcium and magnesium (Fig. 8).

The calcium versus phosphorus plot (Fig. 9) had patterns similar to those for the calcium versus magnesium plot (Fig. 8). Endocuticle nonsuture and exocuticle nonsuture had comparable calcium concentrations, but exocuticle nonsuture had a significantly greater phosphorus concentration than the endocuticle nonsuture (Table 2), thus leading to a significantly higher Ca/P ratio (Table 4). Exocuticle nonsuture had the lowest calcium to phosphorus (Ca/P) ratio, which was significantly different from all the other regions with the exception of lower endocuticle suture (Table 4). Endocuticle nonsuture had the highest Ca/P ratio, which was significantly different from all other re-

gions. The remaining regions had Ca/P ratios significantly different from each other and from lower endocuticle suture and exocuticle nonsuture (Table 4). Again, a positive relationship was seen for calcium and phosphorus concentrations in the upper and lower endocuticle suture and exocuticle suture (Fig. 9) but more so for lower endocuticle suture and exocuticle suture, whose distributions overlapped. Values for upper endocuticle suture clustered between the endocuticle nonsuture values and values for the lower endocuticle suture and exocuticle suture (Fig. 9) and were significantly different from all other regions (Table 4). A few values for lower endocuticle suture clustered closer to zero. Control (resin) values clustered tightly near zero, with no calcium and very little phosphorus (Fig. 9).

DISCUSSION

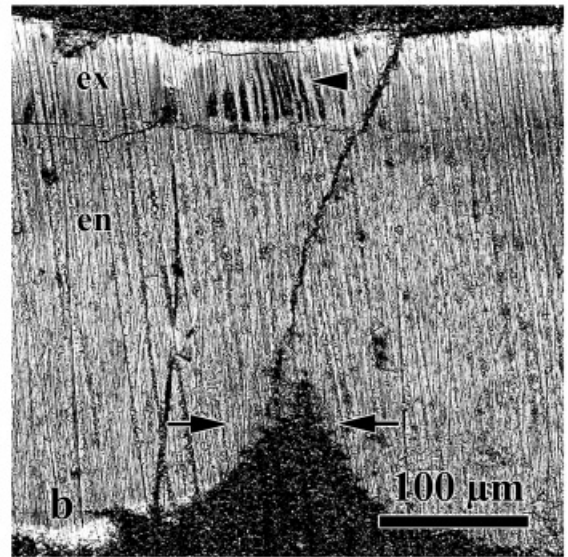
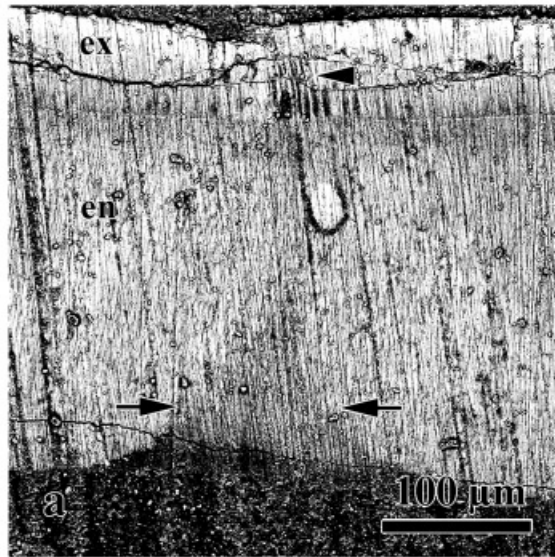
This investigation has revealed several unique features of the ventral suture of the blue crab, *Callinectes sapidus*, which may contribute to creating the predetermined “lines of weakness” (Mangum, 1985) that subsequently lead to the splitting of the cuticle prior to ecdysis. Although the suture morphology and the nature of its organic and inorganic components were in general very similar to that of the adjacent fully calcified cuticle, there were minor, but important, differences in the glycoproteins present and the extent of calcification. The suture was also notably thinner in the posterior portion of the carapace, making it more likely to split first (Figs. 4, 5). Finally, the Ca/Mg ratio and Ca/P ratio in the suture differed from the adjacent calcified cuticle (Figs. 8, 9; Tables 3, 4), which potentially made the mineral of the suture more soluble than that of the adjacent calcified cuticle, as will be discussed below.

The general histological and histochemical techniques used in this investigation were not able to differentiate the suture from the adjacent, nonsuture calcified cuticle. When stained with acridine orange, H&E, PAS, PAF, and toluidine blue, the suture stained the same as the nonsuture calcified cuticle. Because hematoxylin and eosin are sensitive to acidic and basic to neutral moieties, respectively (Presnell & Schreibman, 1997), the relative concentration of acidic and basic to neutral molecules in the layers of the calcified cuticle and suture are very similar. This is in striking contrast to the situation in the arthroal membrane (Williams et al., 2003), which stains very differently from the calcified

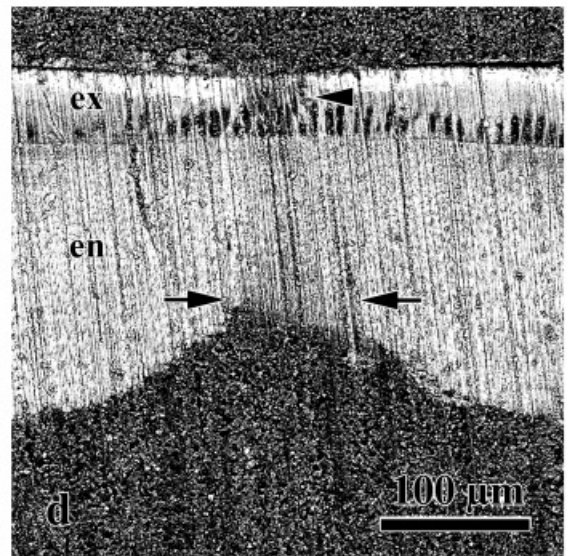
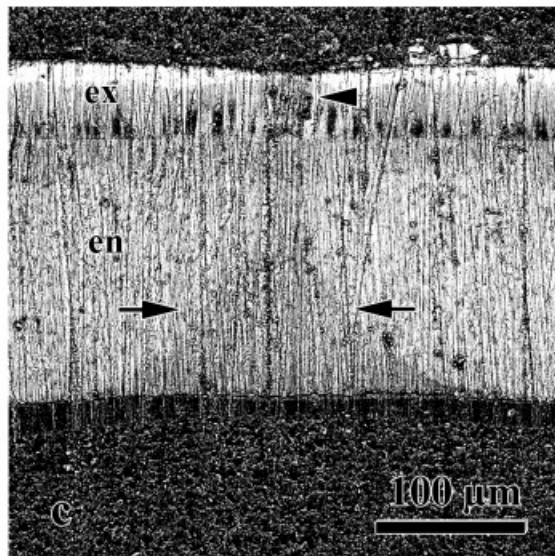
early D₂

late D₂

anterior



middle



posterior

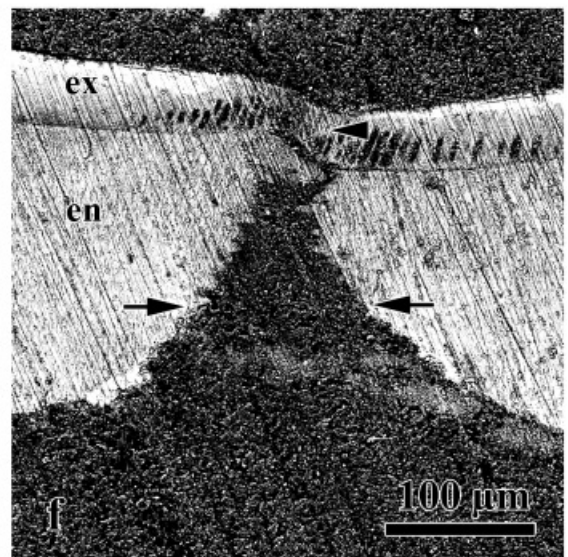
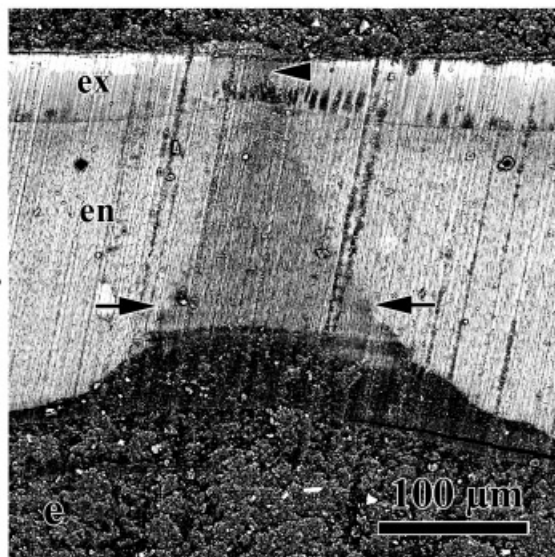


Figure 5. BSE micrographs of embedded and cut samples containing the suture of crabs in early and late D₂ stages. Arrows: suture region of the endocuticle; arrowheads: suture region of the exocuticle; en: endocuticle; ex: indicates exocuticle.

cuticle. In the arthroal membrane the region adjacent to the exocuticle is eosinophilic whereas the exocuticle of the calcified cuticle is strongly basophilic. The suture was also not differentiated by PAS staining, which was used to demonstrate that the pre-exuvial and post-exuvial cuticle of the arthroal membrane was contiguous with the exocuticle and endocuticle of the calcified cuticle (Williams et al., 2003). The PAS reaction is dependent on sugars, with adjacent hydroxyls reacting with Schiff reagent after being oxidized to dialdehydes with periodic acid (Thompson, 1966; Presnell & Schreibman, 1997). The inability of PAS to differentiate the suture from the adjacent calcified cuticle indicates that any differences in the concentration of these moieties within the suture were so slight as to be undetectable. When sections were treated with amylase, PAS staining was noticeably decreased in the exocuticle, suggesting that molecules containing β -1,4-glucose moieties might be present. However, the location of the suture was not revealed by amylase treatment either.

Staining with PAF reveals sulfhydryl-containing molecules in tissue sections (Gomori, 1950). Such sulfhydryl-containing molecules have been localized in bovine growth plate by Byers et al. (1997) and in cementum and dentine by McKee et al. (1996), where they have been suggested to have a role in mineralization. Both the exocuticle and endocuticle stained moderate to lightly with PAF, with little difference between the two layers. Furthermore, the suture was not detectable, suggesting that although sulfhydryl-containing molecules might represent a minor component of the cuticle, they do not seem to contribute to any differences between the suture and the adjacent calcified cuticle.

Acridine orange is a fluorescent cationic dye that has been used to clearly differentiate all four layers of the cuticle in *C. sapidus*, supposedly binding to glycoproteins or glucosaminoglycans (Marlowe & Dillaman, 1995). The metachromatic fluorescence demonstrated by the dye in this application seems to indicate variable concentrations of those molecules in the different layers of the cuticle (Fig. 1a). The inability of this stain to differentiate the suture from the adjacent calcified cuticle would once again suggest that any differences in the relative concentrations of these moieties between the two regions are so slight as to be undetectable.

Toluidine blue buffered to pH 9.0 is a general stain that will bind to molecules with an isoelectric point below 9.0, making it a useful histological stain for both chitin and a wide range of cytoplasmic proteins (Thompson, 1966; Presnell & Schreibman, 1997). Although this stain bound

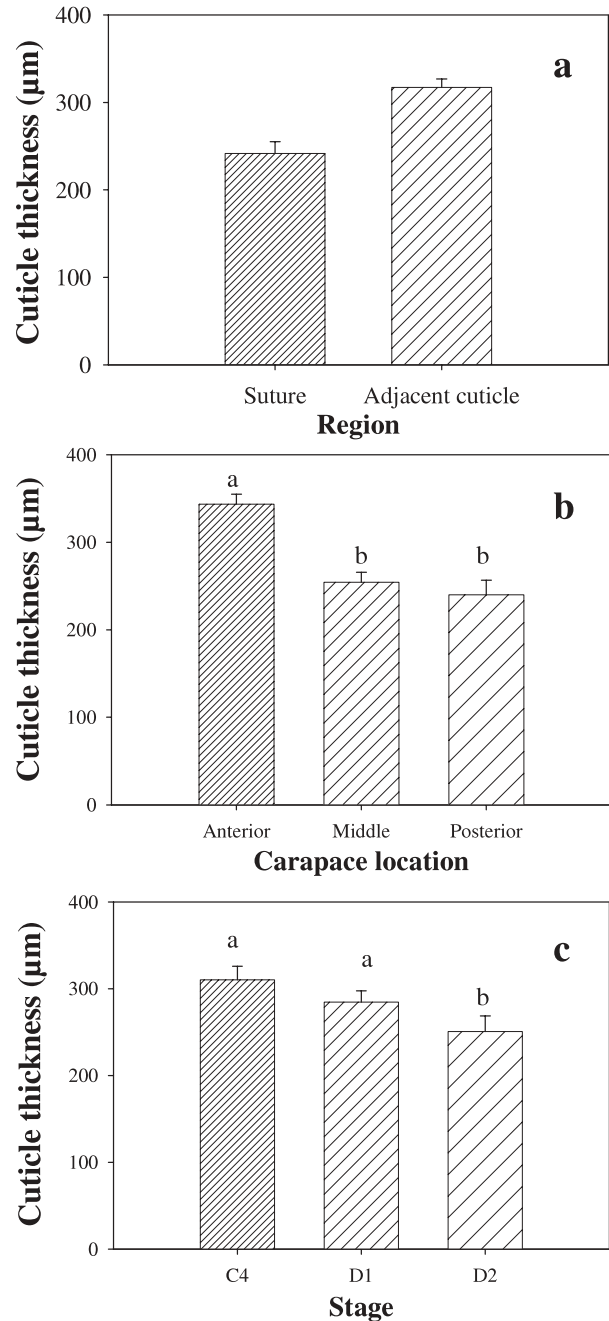


Figure 6. Mean cuticle thickness (in microns; \pm SEM) versus (a) region of the cuticle, (b) carapace location, and (c) stage of the molt cycle. Sample size = 66. Lower case letters (a or b) above bars in panels b and c indicate significant differences in carapace thickness among measurement locations and molt stages based on Tukey HSD post hoc comparisons.

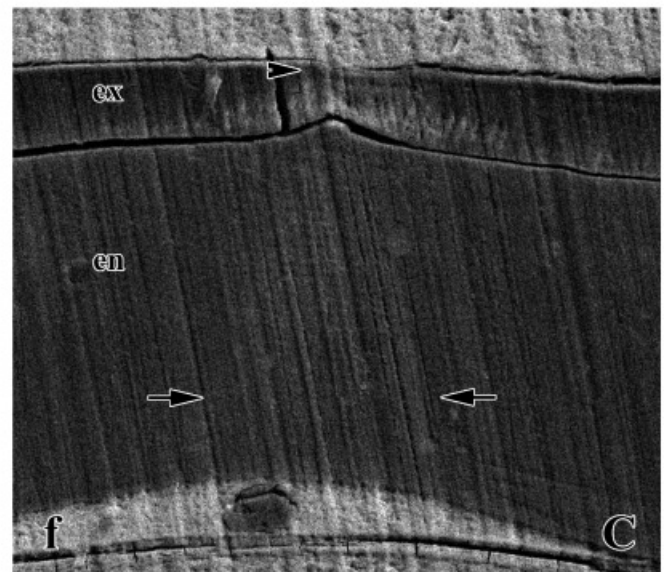
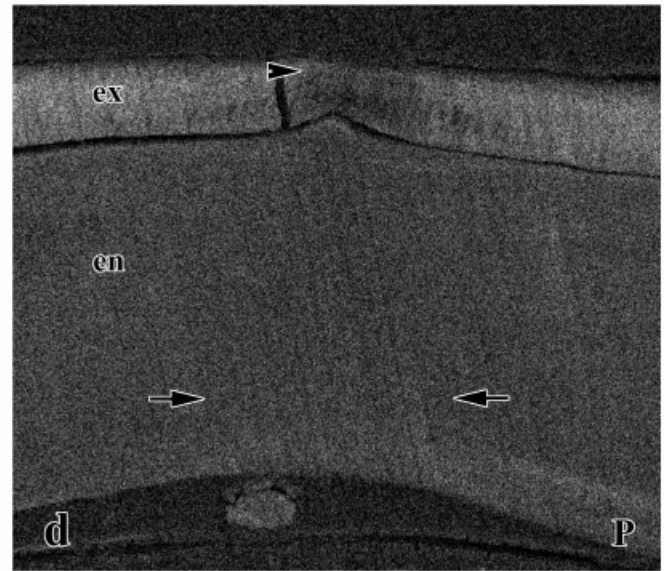
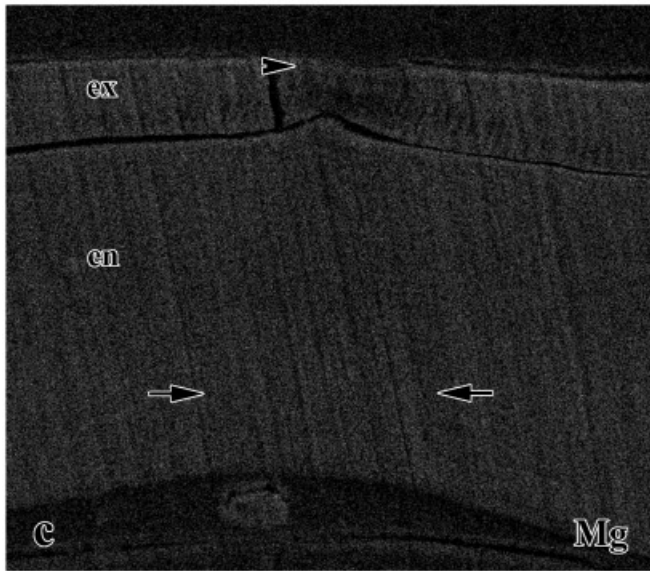
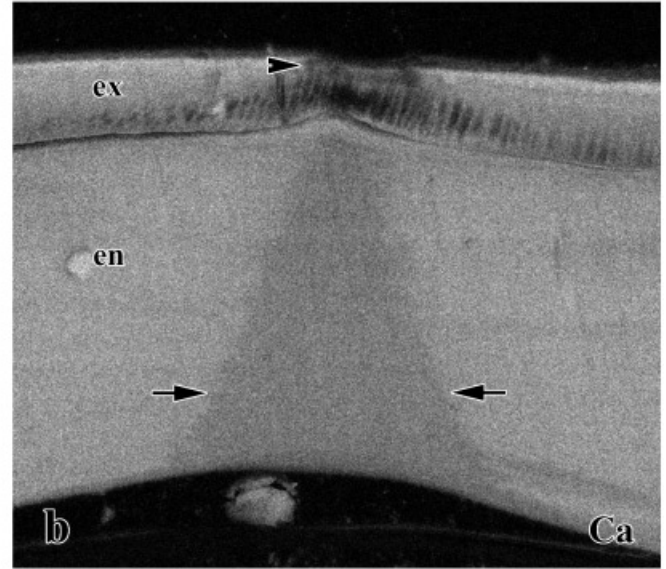
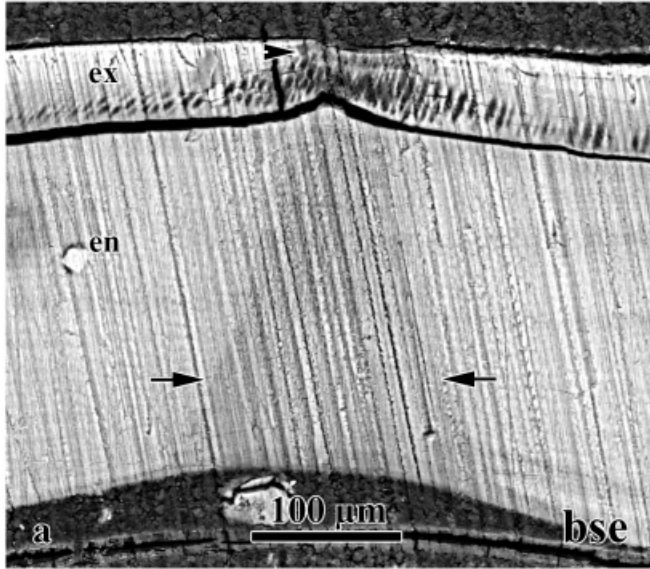


Figure 7. X-ray maps of an embedded posterior piece of cuticle from an intermolt crab containing the suture. Elements mapped were (b) calcium, (c) magnesium, (d) phosphorus, (e) oxygen, and (f) carbon. a: BSE image of the region mapped. Arrows: suture region of the endocuticle; arrowheads: suture region of the exocuticle; en: endocuticle; ex: exocuticle.

Table 1. Concentration (Wt%) of Elements in Suture and Adjacent Cuticle Regions for Molt Stages C₄–D₃ (mean ± SD)

Regions	N	Elements (wt%)				
		Ca	Mg	P	O	C
Endocuticle nonsuture	38	23.42 ± 1.68	1.31 ± 0.14	1.17 ± 0.23	27.29 ± 1.53	33.17 ± 2.41
Upper endocuticle suture	30	17.29 ± 2.89	0.96 ± 0.20	1.05 ± 0.18	23.00 ± 2.53	43.62 ± 5.54
Lower endocuticle suture	33	10.38 ± 7.44	0.66 ± 0.45	0.99 ± 0.50	18.56 ± 6.71	55.19 ± 15.15
Exocuticle nonsuture	41	22.26 ± 1.69	1.75 ± 0.24	2.90 ± 0.50	28.84 ± 1.79	30.40 ± 3.54
Exocuticle suture	38	13.15 ± 3.61	0.86 ± 0.29	1.21 ± 0.35	19.71 ± 3.10	51.43 ± 6.84

Table 2. Statistical Analysis of Elemental Concentrations among Regions of the Cuticle (See Table 1 for Values)

Regions	Elements				
	Ca	Mg	P	O	C
Endocuticle nonsuture vs. upper endocuticle suture	↑ ***	↑ ***	N.D.	↑ ***	↓ ***
Endocuticle nonsuture vs. lower endocuticle suture	↑ ***	↑ ***	N.D.	↑ ***	↓ ***
Endocuticle nonsuture vs. exocuticle nonsuture	N.D.	↓ ***	↓ ***	N.D.	N.D.
Endocuticle nonsuture vs. exocuticle suture	↑ ***	↑ ***	N.D.	↑ ***	↓ ***
Upper endocuticle suture vs. lower endocuticle suture	↑ ***	↑ ***	N.D.	↑ ***	↓ ***
Upper endocuticle suture vs. exocuticle nonsuture	↓ ***	↓ ***	↓ ***	↓ ***	↑ ***
Upper endocuticle suture vs. exocuticle suture	↑ ***	N.D.	N.D.	↑ **	↓ ***
Lower endocuticle suture vs. exocuticle nonsuture	↓ ***	↓ ***	↓ ***	↓ ***	↑ ***
Lower endocuticle suture vs. exocuticle suture	↓ *	↓ *	N.D.	N.D.	N.D.
Exocuticle nonsuture vs. exocuticle suture	↑ ***	↑ ***	↓ ***	↑ ***	↓ ***

***Significantly different ($p < 0.001$); **significantly different ($p < 0.005$); *significantly different ($p < 0.05$); N.D.: not significantly different. Arrow indicates relative concentration of first to second element (↑ = higher, ↓ = lower).

much more intensely to the exocuticle, it was not able to differentiate the suture from the surrounding calcified cuticle.

In summary, the stains used in this investigation only identified categories of molecules within the cuticle, and although they were capable of differentiating individual layers within the cuticle, none was able to differentiate the suture from the surrounding calcified cuticle. Furthermore, the major structural features of the cuticle, namely the thickness and arrangement of the lamella, gave no clue as to the location of the suture. In the puparium cap of the insect *Elenchus tenuicornis*, Kathirithamby et al. (1990) have described the line of weakness as having lamellae with an “open texture” as compared to the adjacent cuticle with densely staining and compact lamellae. They further suggested that the open texture was due to the absence of

tanning in the line of weakness. The absence of any difference of lamellar density and thickness in the suture of the blue crab suggests that there is little difference in composition or tanning of the two regions. Although tanning in crustaceans has been suggested by several authors (Dennell, 1947; Summers, 1967, 1968; Vacca & Fingerma, 1975; Roer & Dillaman, 1993), evidence for the timing or presence of this process in the various regions of the cuticle has not been as well documented as in other arthropods (Hackman, 1984). Taken together, these histochemical and anatomical observations indicate that the structure and general composition of the suture and adjacent calcified cuticle are virtually identical.

Lectins are a diverse group of molecules that have binding affinities for particular carbohydrate moieties. Al-

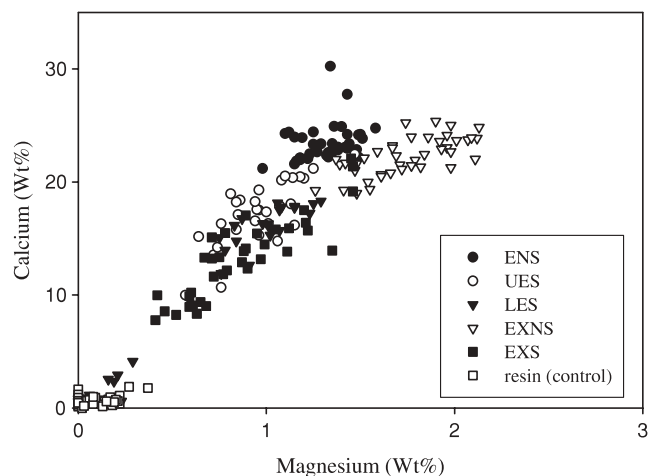


Figure 8. Plots of calcium concentrations (wt%) among cuticle regions against magnesium concentrations (wt%). ENS: endocuticle nonsuture, UES: upper endocuticle of the suture, LES: lower endocuticle of the suture, EXNS: exocuticle nonsuture, EXS: exocuticle of the suture.

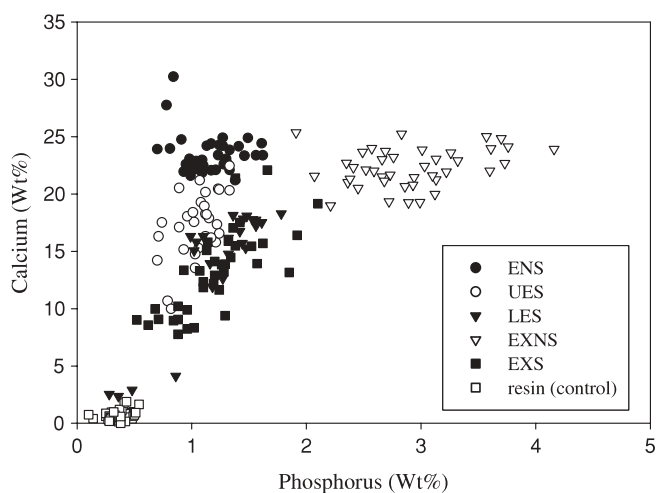


Figure 9. Plots of calcium concentrations (wt%) among cuticle regions against phosphorus concentrations (wt%). ENS: endocuticle nonsuture, UES: upper endocuticle of the suture, LES: lower endocuticle of the suture, EXNS: exocuticle nonsuture, EXS: exocuticle of the suture.

though the specificity of individual lectins can vary considerably, they have proven useful as histochemical probes (Leiner et al., 1986; Spicer & Schulte, 1992). Marlowe et al. (1994) used a battery of 21 different lectins to characterize the composition of the cuticle of *C. sapidus* at various stages of the molt cycle. Of this original battery of 21 lectins, 19 showed no difference between suture and adjacent calcified cuticle, suggesting a quite similar proteoglycan and glycoprotein content. However, two lectins from the original battery (LCA and PSA), as well as VFA, an additional lectin not

Table 3. Mean Values for the Ratios (Mean \pm SD) of Ca/Mg at the Different Cuticle Regions

Regions	Ratios (Mean \pm SD)	Regions				
		ENS	UES	LES	EXNS	EXS
ENS	18.0 (± 1.9)					
UES	N.D.		18.2 (± 2.5)			
LES	***	***		14.5 (± 4.4)		
EXNS	***	***	N.D.		12.9 (± 1.3)	
EXS	**	**	N.D.	***		15.8 (± 2.7)

Statistical analysis of the ratios among regions is summarized below the mean values. ***Significantly different ($p < 0.001$); **significantly different ($p < 0.005$); *significantly different ($p < 0.05$); N.D.: not significantly different. ENS: endocuticle nonsuture, UES: upper endocuticle of the suture, LES: lower endocuticle of the suture, EXNS: exocuticle nonsuture, EXS: exocuticle of the suture.

Table 4. Mean Values for the Ratios of Ca/P (Mean \pm SD) at the Different Cuticle Regions

Regions	Ratios (Mean \pm SD)	Regions				
		ENS	UES	LES	EXNS	EXS
ENS	21.0 (± 5.3)					
UES	***		16.7 (± 3.0)			
LES	***	***		8.7 (± 4.7)		
EXNS	***	***	N.D.		7.9 (± 1.4)	
EXS	***	***	*	***		11.2 (± 2.3)

Statistical analysis of the ratios among regions is summarized below the mean values. ***significantly different ($p < 0.001$); **significantly different ($p < 0.005$); *significantly different ($p < 0.05$); N.D.: not significantly different. ENS: endocuticle nonsuture, UES = upper endocuticle of the suture, LES: lower endocuticle of the suture, EXNS: exocuticle nonsuture, EXS: exocuticle of the suture.

used by Marlowe et al. (1994), differentiated between the suture and the adjacent calcified cuticle (Fig. 1b,c). The suture was seen as a wedge with a trapezoidal cross section whose boundaries were revealed by more intense staining in the exocuticle of the suture and by reduced staining in the endocuticular region (Fig. 1b,c).

All three of these lectins have been described as binding to fucosylated α -N-acetylglucosamine with mannose den-

drimers (Debray et al., 1981; Young et al., 1996) and therefore indicate the presence of glycoproteins containing these types of oligosaccharides at the sites of intense binding, namely, the exocuticle of the suture and some prisms in the vicinity of the suture. The general binding pattern was the same for the three lectins, but there were some differences in intensity, with VFA binding less intensely than the other two lectins. The differences observed in binding intensity by the three lectins may have been due to steric hindrance, differences in the size of the lectin conjugates, or the quantity of similar, but slightly different, lectin-binding moieties. In addition, it was also observed in this study that fixation with alcoholic formalin favored the retention of the proteoglycans and glycoproteins of interest. Similar results were noted by Marlowe et al. (1994), who also noted intense binding of most lectins in tissue samples fixed in alcoholic formalin. Marlowe et al. (1994) also noted intense staining after fixation with Rossman's fluid, which is also referred to as alcoholic Bouin's. Fixation in aqueous Bouin's, which was used in this study, did not result in similar staining. This suggests that preservation of the oligosaccharides bound by the three lectins is more a function of the alcohol in the fixative than the presence of picric acid, which is the other major element shared by both types of Bouin's fixative.

If the moieties bound by LCA, PSA, and VFA are related to the inhibition of mineralization, the observed staining patterns would predict that the exocuticle of the suture would be much less mineralized than the adjacent calcified exocuticle, but that the endocuticle of the suture would be more calcified than the adjacent endocuticle of the calcified cuticle. However, this assumes that calcification in the exocuticle and endocuticle is identical and that mineralization is regulated in the same manner by the same set of molecules. In fact, calcification in the two major layers is distinctly different (Dillaman et al., 2005). Calcification of the exocuticle occurs after ecdysis on a preformed matrix whereas endocuticle matrix is produced after ecdysis and mineralized as it is deposited (Green & Neff, 1972; Hegdahl et al., 1977a, 1977c). Exocuticle calcification has two phases. The first phase involves the mineralization of the IPS, which starts at the outer and inner boundaries of the exocuticle and then moves toward the middle of the exocuticle (Giraud-Guille, 1984a; Hequembourg, 2002). The initial mineral phase is amorphous calcium carbonate, which later changes into a more stable form of calcium carbonate, calcite (Hequembourg, 2002; Dillaman et al., 2005). The second phase involves infilling of the prisms with mineral. The prisms fill first at the outer exocuticle boundary and mineralization then proceeds inward (Hequembourg, 2002). The glycoproteins bound by LCA, PSA, and VFA may possibly be responsible for regulating the first or second phase of calcification in the exocuticle of the suture. For example, Coblenz et al. (1998) suggested that the removal of glycoproteins after ecdysis was necessary for calcification to occur in the exocuticle. The presence of the LCA-, PSA-, and VFA-binding glycoproteins in the suture exocuticle of intermolt crabs

may indicate that because the glycoproteins were not removed, the cuticle was not calcified. The same interpretation could be extended to the regions of the prisms close to the endocuticle but outside the suture that bound the three lectins.

The vast majority of the lectins used indicated that the carbohydrate composition of the suture is more like than unlike the adjacent calcified cuticle, thereby reinforcing the histology and histochemistry results. However, the three lectins, LCA, PSA, and VFA, were useful for identifying the suture. Furthermore, it is possible that the minor difference in glycoprotein content at the suture may be responsible for making it more susceptible to digestion by the molting fluid, which has been shown morphologically by Compère et al. (1998) and biochemically by Roer et al. (2001) to be selective in its enzymatic breakdown of carbohydrate moieties within the cuticle.

The suture at intermolt is visible to the unaided eye due to the presence of a groove observed internally and externally (Fig. 2a,b) and at low magnification the absence of setae on the exterior of the carapace over the suture (Fig. 3a) makes it obvious as does the presence of a knobbed ridge paralleling the suture on the external surface (Fig. 2a). Because the groove makes the suture thinner, one may assume that it is weaker than the adjacent calcified cuticle. The observed decreases in thickness varied with molt stage and location on the carapace; that is, the suture was thinnest at late premolt and at the posterior aspect of the carapace (Figs. 4, 5e–f, 6b–c). All these characteristics (being thinner than adjacent calcified cuticle, being thinnest at late premolt, and being thinnest at posterior) make the suture mechanically weaker, thereby directing a fracture in a specific location, much like scoring glass (Vogel, 1988). The phenomenon that puts the old cuticle under tension is the rising internal pressure due to the water uptake by the crab prior to ecdysis (Passano, 1960; Green & Neff, 1972; Mangum et al., 1985). The suture preferentially fails (or splits) first at the posterior end of the carapace, so that the crab can crawl backwards out of the old shell or exuvium. Consequently, the anterior portion of the suture, which is only partially digested, acts as a hinge.

The BSE and X-ray analysis showed exactly the same trapezoidal morphology for the suture as the lectin staining revealed (Figs. 4, 5, 7). In a developmental sense, this wedged-shaped pattern suggests that the epithelium depositing the suture is not a fixed number of cells. Because mitosis in the hypodermis precedes the deposition of the cuticle, from D_1 to C_3 , epithelial cells at the margin of the suture must be differentiating from those forming nonsuture calcified cuticle into suture-forming epithelia, in much the same way as previously noted by Williams et al. (2003) in their investigation of the epithelium forming the arthrodistal membrane of the blue crab. Furthermore, because the suture trapezoidal shape varies from anterior to posterior regions of the carapace, the pattern of cell differentiation also varies spatially. As the structure of the nonsuture calcified cuticle and the

suture appear to be so similar, this differentiation may involve simply turning on or off a few genes.

In BSE images the signal is brighter when higher atomic number elements are present (Murphy, 2001). The observed brighter regions in the cuticle were therefore due to mineralization (Figs. 4, 5). This was verified by X-ray mapping (Fig. 7b). In the exocuticle of the suture the bright BSE signal indicated that only the IPS were mineralized (Figs. 4, 5). The prisms were clearly not mineralized in the exocuticle region of the suture and resembled 8-h postmolt exocuticle described by Hequembourg (2002) for mineralized cuticle. This indicates that the initial phase of calcification in the suture exocuticle, the mineralization of the IPS, was not different from that of nonsuture exocuticle. However, the second phase of calcification in the suture, the in-filling of the prisms, was presumably arrested in early postmolt. This appears to be a permanent inhibition of mineralization because when the surface of the suture in fully mineralized intermolt crabs was examined in the BSE mode the suture appeared darker than the adjacent calcified cuticle, suggesting that it has much less mineral than the adjacent cuticle (Fig. 4a,c,e). This was also verified by calcium X-ray mapping (Fig. 7b). Although some of the decrease in the BSE signal could be attributed to the increased distance from the surface of the cuticle to the BSE detector due to the surface groove, the difference in height of the cuticle surface was relatively slight and all surfaces were well within the optimum working distance for the BSE detector (8.5 mm). The calcium map of the cuticle surface in the region of the suture (Fig. 7b) demonstrated that calcium was present in the suture, albeit at lower concentrations.

Back-scattered electron images of the endocuticle as well as X-ray maps revealed that there was slightly less calcium in the suture than in the adjacent calcified cuticle (Figs. 4, 5, 7b). This is inconsistent with the previously stated suggestion that the degree of inhibition of mineralization is directly related to the intensity of lectin staining with LCA, PSA, and VFA. Rather, these observations suggest that these lectins are binding more than one glycoprotein, and that those glycoproteins, while having similar oligosaccharides, would have to have opposite roles, one being an inhibitor of mineralization and the other a promoter. This concept of molecules, including glycoproteins, serving as both inhibitors and promoters of crystal nucleation is not new and has been suggested to occur in many calcifying systems (Crenshaw, 1982; Addadi & Weiner, 1985; Wheeler et al., 1988; Gunthorpe et al., 1990). Addadi and Weiner (1985) stated that nucleation occurred when some proteins were attached to a solid substrate, such as an organic matrix, whereas inhibition occurred when some proteins were not attached but in solution and interacting with the formed crystals.

Secondary electron images supported the information from BSE images and X-ray maps. The matrix fibers of the suture exocuticle were covered with mineral in the IPS, but in the prisms the fibers were clearly visible (Fig. 3c). The

fibers/lamellae were contiguous between the suture and adjacent calcified cuticle, thereby verifying the results of the general histological and histochemical stains. There was no departure from the morphology of the calcified adjacent cuticle. Although the empty prisms allowed one to determine the boundaries of the suture in the exocuticle in the BSE and SE modes, the same was not true for the endocuticle because the difference in the degree of mineralization was so slight in the suture as compared with the adjacent calcified cuticle as to make them indistinguishable even in the BSE mode (Fig. 3b). Taken together, the SE images would suggest mineralization in the endocuticle region of the suture is not qualitatively different from the adjacent calcified cuticle, whereas the mineralization of the exocuticle appears to be incomplete, closely resembling an early stage of mineralization when only the IPS are calcified (approximately 8 h postecdysis) (Dillaman et al., 2005).

Those differences in the elemental composition between regions of the suture and the adjacent calcified cuticle were quantified with X-ray microanalysis (Tables 1, 2). The major observation is that the suture is less mineralized than the adjacent calcified cuticle. In addition, the ratio of minor elements to calcium differed significantly between the suture and adjacent calcified cuticle (Figs. 8, 9; Tables 3, 4). Ratios of minor elements, especially magnesium and phosphorus, in calcified structures have been examined in a variety of structures from bone to shells, and speculations have been made on the effects these minor elements have on the crystal structure and solubility (Crenshaw, 1982; Giraud-Guille & Quintana, 1982; Compère et al., 1993; Raz et al., 2002). All regions of the suture had a significantly lower relative concentration of magnesium and phosphorus as compared to the adjacent calcified cuticle (Tables 1, 2). As described by Stumm and Morgan (1981), high magnesium calcites, in the range encountered in the cuticle, have a lower solubility, which would render the calcified cuticle less soluble than the suture, therefore making the suture more susceptible to digestion by molting fluid. There may be multiple roles for magnesium and phosphate in the cuticle. It has been reported that both magnesium (Aizenberg et al., 2001) and phosphorus (Levi-Kalishman et al., 2000) stabilize the amorphous calcium carbonate in ascidian spicules. Because amorphous calcium carbonate is also present in nonsuture calcified cuticle (Vinogradov, 1953; Lowenstam & Weiner, 1989; Dillaman et al., 2005), it is possible that the blue crab may be making slight modifications in the mechanisms for regulating mineralization in order to effect a difference in mineral solubility. The preferential thinning of the suture during premolt appears to be due to demineralization followed by partial digestion of the organic matrix. The mineral concentration seemed to gradually decline throughout premolt stages, leaving an organic layer on the inner surface of the cuticle, referred to as "ecdysial membrane" by Compère et al. (1998). Measurements for the lower endocuticle suture were taken where this gradual demineralization of the suture first occurred, so

the lower endocuticle suture displayed a wide range of calcium concentrations. This range would presumably reflect the transition from mineralized to unmineralized matrix. A similar distribution of calcium concentrations in the exocuticle suture suggests a similar process may be occurring.

CONCLUSIONS

In summary, the first hypothesis, that the ventral suture line morphology does not vary from that of the calcified cuticle surrounding it, was not supported with respect to thickness and external morphology. However, the hypothesis was supported with respect to histological features, particularly the structure of the lamellae in the suture, which were indistinguishable from and contiguous with those in the calcified cuticle. Consequently, the suture in *C. sapidus* seems very different from the descriptions (albeit limited) of suture regions in insects (Chapman, 1982; Kathirithamby et al., 1990; Hadley, 1994). The second hypothesis, that the organic matrix of the suture line of crustaceans has the same composition as the adjacent calcified cuticle, was also supported in great measure, with several general histological and histochemical stains being unable to differentiate the two regions. However, although lectin histochemistry for the most part also demonstrated similarities, three lectins out of the 22 were able to clearly differentiate the suture region. The binding by the three lectins, *Lens culinaris* agglutinin, *Pisum sativum* agglutinin, and *Vicia faba* agglutinin, suggested a group of glycoproteins with similar oligosaccharides that may have very different effects on calcification in the two major calcified layers of the suture. In the exocuticle the glycoproteins may be responsible for blocking the second phase of calcification whereas in the endocuticle they may be responsible for normal calcification. The third hypothesis, that the mineral content of the suture does not vary from that of the surrounding calcified cuticle, was clearly rejected. The suture exocuticle and endocuticle were both significantly less calcified than the adjacent calcified cuticle, thereby potentially making it easier to dissolve prior to ecdysis. In addition, the suture also had a higher calcium to magnesium and calcium to phosphate ratio than the adjacent calcified cuticle, making it potentially more soluble and therefore more susceptible to digestion by molting fluid. The fourth hypothesis was also rejected. The suture did vary in dimensions among locations. The combination of wider and thinner suture at the posterior portion of the dorsal carapace makes it more susceptible to digestion, allowing the posterior portion of the suture to be digested first and the anterior portion to act as a hinge. Furthermore, the wedge-shaped nature of the suture is consistent with the concept that the outward force resulting from the swelling of the underlying new cuticle would put the suture exocuticle under tension and the suture endocuticle under compression. Taken altogether, the subtle differ-

ences in matrix composition, mineral concentration and composition, and decreased thickness in prescribed regions make the suture less stable and mechanically weaker, thus predisposing it to fail and thereby assuring successful ecdysis.

ACKNOWLEDGMENTS

Funding for this project was provided by a Sigma Xi Grant-in-Aid of Research to C.P. and National Science Foundation Grants IBN-0114597 and DBI-9978614 to R.M.D. This project was also supported by instrumentation grants to R.M.D.: ONR 99-1-0690, NSF DBI-9970099, NC Biotechnology Center 9903-IDG-1014. We thank Dr. Fred Scharf for the assistance with the data analysis and Drs. Shelly Etnier and Ann Pabst for discussions on biomechanics.

REFERENCES

- ADDADI, L. & WEINER, S. (1985). Interactions between acidic proteins and crystals: Stereochemical requirements in biomineralization. *Proc Natl Acad Sci USA* **82**, 4110–4114.
- AIZENBERG, J., LAMBERT, G., WEINER, S. & ADDADI, L. (2001). Factors involved in the formation of amorphous and crystalline calcium carbonate: A study of an ascidian skeleton. *J Am Chem Soc* **124**, 32–39.
- BUCHHOLZ, F. (1989). Moulting cycle and seasonal activities of chitinolytic enzymes in the integument and digestive tract of the Antarctic krill, *Euphausia superba*. *Polar Biol* **9**, 311–317.
- BYERS, S., VAN ROODEN, J.C. & FOSTER, B.K. (1997). Structural changes in the large proteoglycans, aggrecan, in different zones of the ovine growth plate. *Calcif Tissue Int* **60**, 71–78.
- CHAPMAN, R.F. (1982). *The Insects: Structure and Function*. Cambridge, MA: Harvard University Press.
- COBLENTZ, F.E., SHAFER, T.H. & ROER, R.D. (1998). Cuticular proteins from the blue crab alter *in vitro* calcium carbonate mineralization. *Comp Biochem Physiol B: Biochem Mol Biol* **121**, 349–360.
- COMPÈRE, P. & GOFFINET, G. (1987a). Ultrastructural shape and three-dimensional organization of the intracuticular canal systems in the mineralized cuticle of the green crab, *Carcinus maenas*. *Tissue & Cell* **19**, 839–857.
- COMPÈRE, P. & GOFFINET, G. (1987b). Elaboration and ultrastructural changes in the pore canal system of the mineralized cuticle of *Carcinus maenas* during the molting cycle. *Tissue Cell* **19**, 859–875.
- COMPÈRE, P., MORGAN, J.A. & GOFFINET, G. (1993). Ultrastructural location of calcium and magnesium during mineralization of the cuticle of the shore crab, as determined by the K-pyroantimonate method and X-ray microanalysis. *Cell Tissue Res* **274**, 567–577.
- COMPÈRE, P., THOREZ, A. & GOFFINET, G. (1998). Fine structural survey of the old cuticle degradation during pre-ecdysis in two European Atlantic crabs. *Tissue Cell* **30**, 41–56.
- CRENSHAW, M.A. (1982). Biological mineralization and demineralization: Mechanisms of normal biological mineralization of

- calcium carbonates. In *Dahlem Konferenzen*, Nancollas, G.H. (Ed.), pp. 243–257. New York: Springer-Verlag.
- DEBRAY, H., DECOUT, D., STRECKER, G., SPIK, G. & MONTREUIL, J. (1981). Specificity of twelve lectins towards oligosaccharides and glycopeptides related to *N*-glycosylproteins. *Eur J Biochem* **117**, 41–55.
- DENNEL, R. (1947). The occurrence and significance of phenolic hardening in the newly formed cuticle of Crustacea Decapoda. *Proc R Soc Lond B Biol Sci* **134**, 485–503.
- DILLAMAN, R., HEQUEMBOURG, S. & GAY, M. (2005). Early pattern of calcification in the dorsal carapace of the blue crab, *Callinectes sapidus*. *J Morphol* **263**, 356–374.
- DRACH, P. (1939). Mue et cycle d'intermue chez les crustacés décapodes. *Ann Inst Oceanogr* **19**, 103–391.
- FREEMAN, J.A. (1980). Hormonal control of chitinolytic activity in the integument of *Balanus amphitrite*, *in vitro*. *Comp Biochem Physiol A Physiol* **65**, 13–17.
- GIRAUD-GUILLE, M.M. (1984a). Calcification initiation sites in the crab cuticle: The interprismatic septa, an ultrastructural cytochemical study. *Cell Tissue Res* **236**, 413–420.
- GIRAUD-GUILLE, M.M. (1984b). Fine structure of the chitin-protein system in the crab cuticle. *Tissue Cell* **16**, 75–92.
- GIRAUD-GUILLE, M.M. & QUINTANA, C. (1982). Secondary ion microanalysis of the crab calcified cuticle: Distribution of mineral elements and interactions with cholesteric organic matrix. *Biol Cell* **44**, 57–67.
- GOMORI, G. (1950). A new stain for elastic tissue. *Am J Clin Pathol* **20**, 665–666.
- GREEN, J.P. & NEFF, M.R. (1972). A survey of the fine structure of the integument of the fiddler crab. *Tissue Cell* **4**, 137–171.
- GUNTORPE, M.E., SIKES, C.S. & WHEELER, A.P. (1990). Promotion and inhibition of calcium carbonate crystallization *in vitro* by matrix protein from blue crab exoskeleton. *Biol Bull* **179**, 191–200.
- HACKMAN, R.H. (1984). Cuticle: Biochemistry. In *Biology of the Integument 1: Invertebrates*, Bereiter-Hahn, J., Matoltsy, A.G. & Richards, K.S. (Eds.), pp. 583–610. Berlin: Springer-Verlag.
- HADLEY, N.F. (1994). *Water Relations of Terrestrial Arthropods*. San Diego, CA: Academic Press.
- HEGDAHL, T., GUSTAVSEN, F. & SILNESS, J. (1977a). The structure and mineralization of the carapace of the crab (*Cancer pagurus* L.): The exocuticle. *Zool Scr* **6**, 101–105.
- HEGDAHL, T., GUSTAVSEN, F. & SILNESS, J. (1977b). The structure and mineralization of the carapace of the crab (*Cancer pagurus* L.): The epicuticle. *Zool Scr* **6**, 215–220.
- HEGDAHL, T., SILNESS, J. & GUSTAVSEN, F. (1977c). The structure and mineralization of the carapace of the crab (*Cancer pagurus* L.): The endocuticle. *Zool Scr* **6**, 89–99.
- HEQUEMBOURG, S.J. (2002). Early patterns of calcium and protein deposition in the carapace of the blue crab. M.S. Thesis. University of North Carolina at Wilmington.
- JOHNSON, P.T. (1980). *Histology of the Blue Crab, Callinectes sapidus. A Model of the Decapoda*. New York: Praeger Publishers.
- KATHIRITHAMBY, J., LUKE, B.M. & NEVILLE, A.C. (1990). The ultrastructure of the preformed ecdysial 'line of weakness' in the puparium cap of *Elenchus tenuicornis* (Kirby) (Insecta: Strepsiptera). *Zool J Linnean Soc* **98**, 229–236.
- LEINER, I.E., SHARON, H. & GOLDSTEIN, I.J. (Eds.). (1986). *The Lectins. Properties, Functions, and Applications in Biology and Medicine*. Orlando, FL: Academic Press.
- LEVI-KALISMAN, Y., RAZ, S., WEINER, S., ADDADI, L. & SAGI, I. (2000). X-ray absorption spectroscopy studies on the structure of a biogenic "amorphous" calcium carbonate phase. *J Chem Soc/Dalton Trans* **2000**, 3977–3982.
- LOWENSTAM, H.A. & WEINER, S. (1989). *On Biomineralization*. New York: Oxford University Press.
- MANGUM, C.P. (1985). Molting in the blue crab *Callinectes sapidus*: A collaborative study of intermediary metabolism, respiration and cardiovascular function, and ion transport. Preface. *J Crustacean Biol* **5**, 185–187.
- MANGUM, C.P., DEFUR, P.L., FIELDS, J.H.A., HENRY, R.P., KORMANIK, G.A., MCMAHON, B.R., RICCI, J., TOWLE, D.W. & WHEATLY, M.G. (1985). Physiology of the blue crab *Callinectes sapidus* Rathbun during a molt. *National Symposium on the Soft-Shelled Blue Crab Fishery*, February 12–13, pp. 1–12.
- MARLOWE, R.L. & DILLAMAN, R.M. (1995). Acridine orange staining of decapod crustacean cuticle. *Invertebr Biol* **114**, 79–82.
- MARLOWE, R.L., DILLAMAN, R.M. & ROER, R.D. (1994). Lectin binding by crustacean cuticle: The cuticle of *Callinectes sapidus* throughout the molt cycle, and the intermolt cuticle of *Procambarus clarkii* and *Ocypode quadrata*. *J Crustacean Biol* **14**, 231–246.
- McKEE, M.D., ZALZAL, S. & NANJI, A. (1996). Extracellular matrix in tooth cementum and mantle dentin: Localization of osteopontin and other noncollagenous proteins, plasma proteins, and glycoconjugates by electron microscopy. *Anat Rec* **245**, 293–312.
- MURPHY, D.B. (2001). *Fundamentals of Light Microscopy and Electron Imaging*. New York: Wiley-Liss.
- NEVILLE, A.C. (1975). *Zoophysiology and Ecology, vol. 4/5: Biology of the Arthropod Cuticle*, Hoar, W.S., Jacobs, J., Langer, H. & Lindauer, M. (Eds.). New York: Springer-Verlag.
- O'BRIEN, J.J. & SKINNER, D.M. (1987). Characterization of enzymes that degrade crab exoskeleton: I. Two alkaline cysteine proteinase activities. *J Exp Zool* **243**, 389–400.
- O'BRIEN, J.J. & SKINNER, D.M. (1988). Characterization of enzymes that degrade crab exoskeleton: II. Two acid proteinase activities. *J Exp Zool* **246**, 124–131.
- PASSANO, L.M. (1960). Molting and its control. In *The Physiology of Crustacea. Volume 1: Metabolism and Growth*, Waterman, T. (Ed.), pp. 473–536. New York: Academic Press.
- PRESNELL, J.K. & SCHREIBMAN, M.P. (1997). *Humason's Animal Tissue Techniques*. Baltimore, MD: The Johns Hopkins University Press.
- RASCH, R., CRIBB, B.W., BARRY, J. & PALMER, C.M. (2003). Application of quantitative analytical electron microscopy to the mineral content of insect cuticle. *Microsc Microanal* **9**, 152–154.
- RAZ, S., TESTENIERE, O., HECKER, A., WEINER, S. & LUQUET, G. (2002). Stable amorphous calcium carbonate is the main component of the calcium storage structures of the crustacean *Orchestia cavimana*. *Biol Bull* **203**, 269–274.
- RAZ, S., WEINER, S. & ADDADI, L. (2000). Formation of high magnesium calcites via and amorphous precursor phase: Possible biological implications. *Adv Mater* **12**, 38–42.
- REDDY, G.H. & NANCOLLAS, G.H. (1976). The crystallization of calcium carbonate. IV. The effect of magnesium, strontium and sulfate ions. *J Crystal Growth* **35**, 33–38.
- ROER, R.D. (1980). Mechanisms of resorption and deposition of calcium in the carapace of the crab *Carcinus meanas*. *J Exp Biol* **88**, 205–218.

- ROER, R.D. & DILLAMAN, R.M. (1984). The structure and calcification of the crustacean cuticle. *Am Zool* **24**, 893–909.
- ROER, R.D. & DILLAMAN, R.M. (1993). Molt-related change in integumental structure and function. In *The Crustacean Integument: Morphology and Biochemistry*, Horst, M.N. & Freeman, J.A. (Eds.), pp. 1–37. Boca Raton, FL: CRC Press.
- ROER, R.D., HALBROOK, K.E. & SHAFER, T.H. (2001). Glycosidase activity in the post ecdysial cuticle of the blue crab, *Callinectes sapidus*. *Comp Biochem Physiol B Biochem Mol Biol* **128**, 683–690.
- SHAFER, T.H., ROER, R.D., MIDGETTE-LUTHER, C. & BROOKINS, T.A. (1995). Postecdysial cuticle alteration in the blue crab, *Callinectes sapidus*: Synchronous changes in glycoproteins and mineral nucleation. *J Exp Zool* **271**, 171–182.
- SIMKISS, K. (1975). *Bone and Biomineralization*. Studies in Biology no. 53. London: Edward Arnold Publishers Ltd.
- SIMKISS, K. (1994). Amorphous minerals in biology. In *Biomineralization 93. Proceedings of the Seventh International Biomineralization Symposium*. Monaco, November 1993. Allemand, D. & Cuif, J.-P. (Eds). pp. 49–54. Bulletin de l'Institut océanographique, Monaco, n° spécial 14.
- SKINNER, D.M. (1962). The structure and metabolism of a crustacean integumentary tissue during a molt cycle. *Biol Bull* **123**, 635–647.
- SKINNER, D.M. (1985). Molting and regeneration. In *The Biology of Crustacea, vol. 9. Integument, pigments, and hormonal processes*, Bliss, D.E. & Mantel, L.H. (Eds.), pp. 43–146. Orlando, FL: Academic Press, Inc.
- SPICER, S.S. & SCHULTE, B.A. (1992). Diversity of cell glycoconjugates shown histochemically: A perspective. *J Histochem Cytochem* **40**, 1–38.
- SPINDLER, K.D. & BUCHHOLZ, F. (1988). Partial characterization of chitin degrading enzymes from two euphausiids, *Euphausia superba* and *Meganyctiphanes norvegica*. *Polar Biol* **9**, 115–122.
- SPINDLER, K.D. & FUNKE, B. (1989). Characterization of chitinase from the brine shrimp *Artemia*. *Comp Biochem Physiol B Biochem Mol Biol* **94**, 691–695.
- SPINDLER-BARTH, M., VAN WORMHOUDT, A. & SPINDLER, K.D. (1990). Chitinolytic enzymes in the integument and midgut-gland of the shrimp *Palaemon serratus* during the moulting cycle. *Mar Biol* **106**, 49–52.
- SPURR, A.R. (1969). A low viscosity epoxy resin embedding medium for electron microscopy. *J Ultrastruct Res* **26**, 31–43.
- STEVENSON, J.R. (1968). Metecdysial molt staging and changes in the cuticle in the crayfish *Orconectes sanborni* (Faxon). *Crustaceana* **14**, 169–177.
- STEVENSON, J.R. (1972). Changing activities of the crustacean epidermis during the molt cycle. *Am Zool* **12**, 373–380.
- STUMM, W. & MORGAN, J.J. (1981). *Aquatic Chemistry: An Introduction Emphasizing Chemical Equilibria in Natural Waters*. New York: Wiley-Interscience.
- SUMMERS, N.M., JR. (1967). Cuticle sclerotization and blood phenol oxidase in the fiddler crab, *Uca pugnax*. *Comp Biochem Physiol* **23**, 129–138.
- SUMMERS, N.M., JR. (1968). The conversion of tyrosine to catecholamines and the biogenesis of *N*-acetyl-dopamine in isolated epidermis of the fiddler crab, *Uca pugnator*. *Comp Biochem Physiol* **26**, 259–269.
- TAYLOR, J.R.A. & KIER, W.M. (2003). Switching skeletons: Hydrostatic support in molting crabs. *Science* **301**, 209–210.
- THOMPSON, S.W. (1966). *Selected Histochemical and Histopathological Methods*. Springfield, IL: Charles C. Thomas Publisher.
- TRAVIS, D.F. (1955a). The molting cycle of the spiny lobster, *Panulirus argus* Latreille. II. Pre-ecdysial histological and histochemical changes in the hepatopancreas and integumental tissues. *Biol Bull* **108**, 88–112.
- TRAVIS, D.F. (1955b). The molting cycle of the spiny lobster, *Panulirus argus* Latreille. III. Physiological changes which occur in the blood and urine during the normal molting cycle. *Biol Bull* **109**, 484–503.
- TRAVIS, D.F. (1957). The molting cycle of the spiny lobster, *Panulirus argus* Latreille. IV. Post-ecdysial histological and histochemical changes in the hepatopancreas and integumental tissues. *Biol Bull* **113**, 451–479.
- TRAVIS, D.F. (1963). Structural features of mineralization from tissue to macromolecular levels of organization in the decapod Crustacea. *Ann N Y Acad Sci* **109**, 177–245.
- TRAVIS, D.F. (1965). The deposition of skeletal structures in the Crustacea. 5. The histomorphological and histochemical changes associated with the development and calcification of the branchial exoskeleton in the crayfish, *Orconectes virilis* Hagen. *Acta Histochem* **20S**, 193–222.
- TRAVIS, D.F. & FRIBERG, U. (1963). The deposition of skeletal structures in the Crustacea. VI. Microradiographic studies of the exoskeleton of the crayfish *Orconectes virilis* Hagen. *J Ultrastruct Res* **9**, 285–301.
- VACCA, L.L. & FINGERMAN, M. (1975). The mechanisms of tanning in the fiddler crab, *Uca pugnator*. I. Tanning agents and protein carriers in the blood during ecdysis. *Comp Biochem Physiol B Biochem Mol Biol* **51**, 475–481.
- VINOGRADOV, A.P. (1953). *The Elementary Chemical Composition of Marine Organisms*. New Haven, CT: Yale University, Sears Foundation for Marine Research.
- VOGEL, S. (1988). *Life's Devices: The Physical World of Animals and Plants*. Princeton, NJ: Princeton University Press.
- WHEELER, A.P., RUSENKO, K.W., SWIFT, D.M. & SIKES, C.S. (1988). Regulation of *in vitro* and *in vivo* CaCO₃ crystallization by fractions of oyster shell organic matrix. *Mar Biol* **98**, 71–80.
- WILLIAMS, C.L., DILLAMAN, R.M., ELLIOTT, E.A. & GAY, D.M. (2003). Formation of the arthrodiol membrane in the blue crab, *Callinectes sapidus*. *J Morphol* **256**, 260–269.
- YOUNG, N.M., WATSON, D.C. & THIBAUT, P. (1996). Post-translational proteolytic processing and the isolectins of lentil and other Viciae seed lectins. *Glycoconjugate J* **13**, 575–583.
- ZAR, J.H. (1999). *Biostatistical Analysis*, 4th ed. Upper Saddle River, NJ: Prentice-Hall.